

Author Manuscript

Title: Isolation and Structure of Germylene-Germyliumylidenes stabilized by N-Heterocyclic Imine

Authors: Shigeyoshi Inoue; Tibor Szilvási; Daniel Franz; Elisabeth Irran; Tatsumi Ochiai

This is the author manuscript accepted for publication and has undergone full peer review but has not been through the copyediting, typesetting, pagination and proofreading process, which may lead to differences between this version and the Version of Record.

To be cited as: 10.1002/anie.201605636

Link to VoR: <http://dx.doi.org/10.1002/anie.201605636>

Isolation and Structure of Germylene–Germyliumylidenes stabilized by N-Heterocyclic Imine

Tatsumi Ochiai,^[a] Tibor Szilvási,^[b] Daniel Franz,^[c] Elisabeth Irran,^[a] and Shigeyoshi Inoue*^[a,c]

Dedicated to Professor F. Ekkehardt Hahn on the occasion of his 60th birthday

Abstract: The ditopic germanium complex [FGe(NIPr)₂Ge][BF₄] (3[BF₄], IPr = 1,3-bis(2,6-diisopropylphenyl)imidazol-2-ylidene) is prepared by the reaction of the amino(imino)germylene (Me₃Si)₂NGeNIPr (1) with 2 equiv of BF₃·OEt₂. This monocation is converted to the germylene-germyliumylidene 3[BAR^F₄] (Ar^F = 3,5-(CF₃)₂-C₆H₃) by treatment with Na[BAR^F₄]. The tetrafluoroborate salt 3[BF₄] reacts with 2 equiv of Me₃SiOTf to give the novel complex [(OTf)(GeNIPr)₂][OTf] (4[OTf]), which affords 4[BAR^F₄] and 4[Al(OR^F)₄] (R^F = C(CF₃)₃) anion exchange with Na[BAR^F₄] or Ag[Al(OR^F)₄], respectively. The computational, as well as crystallographic study reveals that 4⁺ has significant bis(germyliumylidene) dication character.

Germyliumylidenes, germanium(II) monocations, have been attractive targets for fundamental research because they may exhibit both electrophilic and nucleophilic character.¹ Since the seminal work on the half-sandwich germanocene cation [(η⁵-C₅Me₅)Ge]⁺,² various types of donor-stabilized germyliumylidenes have been reported.³ Of the diverse types of synthetic methods for the preparation of germyliumylidenes that have been studied, the halide abstraction from suitable germylene precursors is found to be the most popular one. For instance, the aminotroponimate Ge(II) monocation **I** was synthesized via removal of chloride from a respective chlorogermylene using (η⁵-C₅H₅)ZrCl₃ as a halide scavenger (Figure 1).^{3a} In another example, chloride abstraction with Li[Al(OR^F)₄] (R^F = C(CF₃)₃) furnished a bulky amide-substituted germyliumylidene.^{3g}

It is reasonable to assume that the cationic charge would increase the electrophilicity of germyliumylidenes as compared to their neutral congeners and render these compounds particularly prone to aggregation. In fact, highly charged dicationic germanium(II) complexes require strong donor ligands and a large coordination number of the metal for isolation.⁴ Accordingly, reports on dicationic bis(germyliumylidene) complexes which comprise two cationic metal atoms in the same

that the stability of such compounds is additionally impaired by severe Coulomb repulsion between the metal centers. In sharp contrast, neutral inter-connected and spacer-separated bis(germylene) compounds have been investigated thoroughly and several representatives of this compound class were described.^{7,8} In addition, the use of bis(germylene) as a chelating ligand towards transition metals⁹ contributed to the development of this field.^{9,10} In fact, some of the reported bis(germylene)-metal complexes, showed pronounced catalytic activity for C–C coupling^{10d} or hydroboration.^{10b}

As an intriguing example as to how charge distribution into the adjacent ligand system can reduce Coulomb repulsion between metal centers serves the dianionic disilicate **II** (Figure 1).⁵ In analogy to this dianionic complex (**II**), Tobita and co-workers synthesized the NHC-stabilized dicationic complexes of type **III** in which the repulsion between the two central germanium atoms is decreased by delocalization of a positive charge into the imidazoline rings (Figure 1).⁶ These complexes (**III**) can be regarded as dimers of the parent metallogermylene monocations with the Ge=Ge double bond.

Since the seminal report on monomeric bis(amido)germylene and stannylene comprising a EN₂Si (E = Ge, Sn, Pb) scaffold by Veith and co-workers (**IV**, Figure 1),¹¹ a rapidly growing number of papers have been published concerning the research on N-heterocyclic metallylenes. Interestingly, the solid structure of the germylene (**IV**) was not reported before 2014.¹²

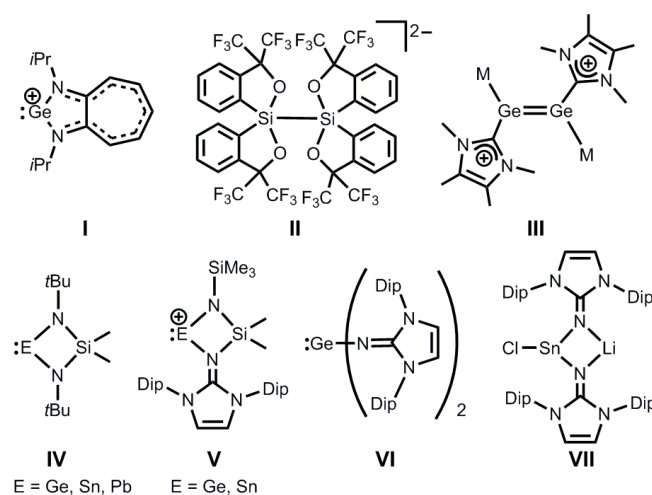


Figure 1. Selected group 14 element compounds: the monocationic germanium(II) compounds **I**, **IV**, **V**, **VI** the dimeric compound (**III**; M = C₅Me₅(CO)₃W), as well as the dianionic disilicate **II** and the stannylene **VII**.

We reported the isolation of the imidazolin-2-imino-substituted Ge(II) and Sn(II) monocations **V** containing a four-membered EN₂Si (E = Ge, Sn) ring system (Figure 1). Their formation is promoted by the delocalization of positive charge density into

[a] MSc. T. Ochiai, Dr. E. Irran, Prof. Dr. S. Inoue
Institut für Chemie, Technische Universität Berlin,
Straße des 17. Juni 135, Sekr. C2, 10623 Berlin (Germany)

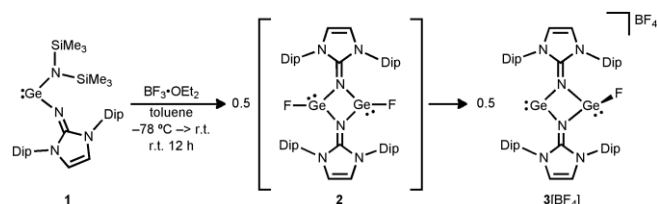
[b] Dr. T. Szilvási
Department of Inorganic and Analytical Chemistry, Budapest
University of Technology and Economics, Szent Gellért tér 4, 1111
Budapest (Hungary).

[c] Dr. D. Franz, Prof. Dr. S. Inoue
Department of Chemistry, Catalysis Research Center and Institute
of Silicon Chemistry, Technische Universität München,
Lichtenbergstraße 4, 85748 Garching (Germany)
E-mail: s.inoue@tum.de

Supporting information for this article is given via a link at the end of the document.

molecule are scarcely found in the literature. One would assume

the imidazoline ring.^{13,14} Notably, this imino system was also implemented in the bis(imino)germylene **VI**¹⁵ and the bis(imino)stannylenoid **VII**¹⁶ and the strongly related imidazolidine-2-iminato ligand has been successfully used for the synthesis of a phosphorus mononitride radical cation.¹⁷ These studies reveal that the imidazolin-2-imino group is particularly efficient in the stabilization of electron-deficient species. Herein we describe the isolation of hitherto unknown cationic germanium heterocycles and a new spacer-separated bis(germylene) bistriflate with pronounced bis(germyliumylidene) character.



Scheme 1. Synthesis of the germyliumylidene salt **3**[BF₄].

Treatment of the amino(imino)germylene **1** with 2 equiv of BF₃·OEt₂ afforded the tetrafluoroborate salt **3**[BF₄] the formation of which proceeds via the intermediate fluorogermylene dimer [FGeNiPr]₂ (**2**) as suggested by DFT calculations (Scheme 1, Figure S35).¹⁸ Thus, the boron trifluoride subsequently assumes the role of a fluorination reagent, as well as a fluoride abstraction agent. The formulation of **3**[BF₄] was confirmed by multinuclear NMR spectroscopy, high resolution mass spectrometry, and X-ray single crystal structure analysis. In the latter we find a highly disordered germanium-bonded fluorine atom which possesses a 50% site-occupancy factor at each of the two Ge-atoms. Due to this disorder, we could not assign the germylene site and the germyliumylidene site in **3**[BF₄].¹⁸

The conversion of **3**[BF₄] with Na[BAr^F₄] (Ar^F = 3,5-bis(trifluoromethyl)phenyl) led to the formation of **3**[BAr^F₄] by anion exchange. In the molecular structure derived from X-ray single crystal analysis the disorder of the Ge-bonded fluorine atom as in **3**[BF₄] is not observed. We find that the cation is marked by a distorted square planar Ge₂N₂ ring as a main structural feature (Figure 2). It exhibits two longer Ge–N_{imine} distances to the Ge1 atom that bears a fluoride substituent (2.025(3) Å, 2.030(3) Å) and two shorter Ge–N_{imine} bond lengths to the Ge2 center (1.876(3) Å, 1.897(3) Å). In compliance with this finding the N1–Ge1–N4 angle of 74.90(11)° is smaller than the N1–Ge2–N4 angle of 81.64(11)°. The Ge–F bond length of 1.800(4) Å falls within the range for germanium–fluorine single bonds.¹⁹ We suggest that the bonding situation in **3**⁺ is described in high approximation by the resonance structure **A1** rather than the formulation **A2** (Scheme 2). The former represents a bis(imino)germylene-stabilized fluorogermlyliumylidene and the latter an iminogermlyliumylidene aggregated with an iminofluorogermlylene via two germanium–nitrogen dative bonds. Interestingly, the coordinating properties of ligand systems that comprise divalent metal atoms of the group 14 elements but bond via adjacent functionalities rather than the ylidenic centers

have scarcely been investigated. Breher and co-workers reported unique bis(stannylenes), where two tin(II) centers are linked head-to-tail via the pyrazole fragments.²⁰ This arrangement is energetically favored over distannene composed of an Sn=Sn double bond. Furthermore, Power and co-workers used the metallylene compound **VIII** for the synthesis of the molybdenum complex **IX** in which the transition metal prefers chelate-fashioned coordination by the two sulfur atoms instead of binding to the low-valent metal center (Scheme 3).²¹ A notable change in the SES fragment (E = Ge or Sn) upon transformation of **VIII** into **IX** is the elongation of the E–S bond with concomitant decrease of the S–E–S bond angle. Accordingly, the Ge2–N_{imine} distances in the ditopic cation **3**⁺ are increased with respect to the monotopic bis(imino)germylene **VI** (1.876(3) Å and 1.897(3) Å vs. 1.8194(15) Å).²¹ Moreover, the N1–Ge2–N4 angle of 81.64(11)° is considerably more acute than the N–Ge–N angle of 99.48(10)° in **VI**. These comparisons between **VIII** and **IX**, as well as **VI** and **3**⁺ affirm the suggested resonance structure **A1** for **3**⁺ with its marked cationic fluorogermlyliumylidene moiety. We conclude that the bis(imino)germylene group functions as a bidentate ligand that bonds to the Ge(II)⁺ center via the nitrogen atoms of the imino functionalities. The efficiency of the bis(imino) group to stabilize the cationic metal center is shown by the C_{NHC}–N_{imine} distances (NHC = N-heterocyclic carbene = imidazoline-2-ylidene) of 1.324(4) Å and 1.334(4) Å in **3**⁺ which exceed the 1.273(2) Å reported for **VI**.¹⁵ The delocalization of positive charge density into the imidazoline ring is illustrated by resonance structure **A3**, as well as **A4** (Scheme 2).

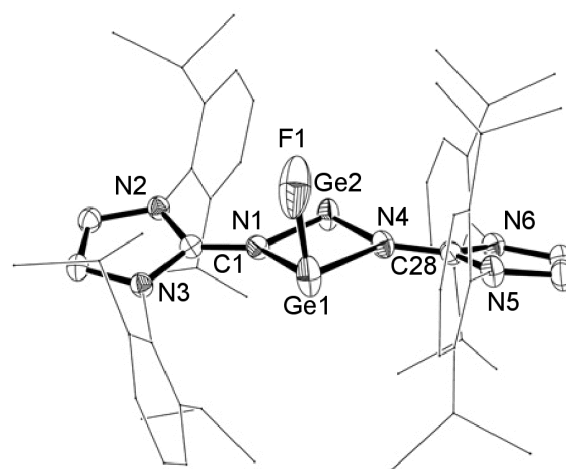
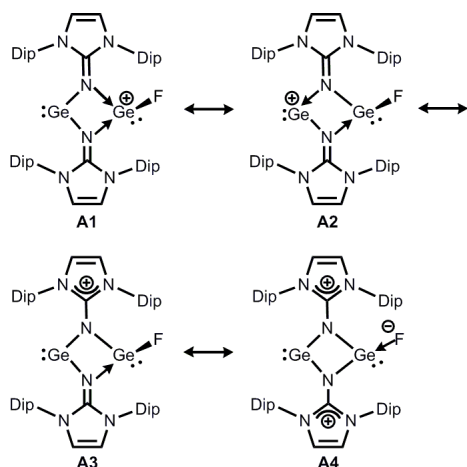
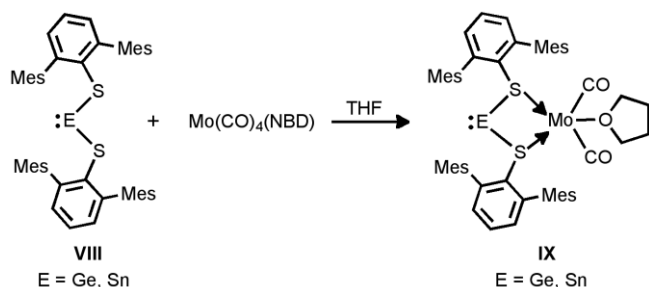


Figure 2. ORTEP representation of the molecular structure of the cation in **3**[BAr^F₄]; The thermal ellipsoids are at the 40% probability level. Hydrogen atoms and solvent molecules are omitted for clarity. For disordered atoms only the higher occupied site is shown. Dip groups are depicted as stick models. Selected bond lengths (Å) and bond angles (deg): Ge1–F1, 1.800(4); Ge1–N1, 2.030(3); Ge1–N4, 2.025(3); Ge2–N1, 1.876(3); Ge2–N4, 1.897(3); N1–C1, 1.324(4); N2–C1, 1.365(4); N3–C1, 1.357(4); N4–C28, 1.334(4); N5–C28, 1.344(5); N6–C28, 1.357(4); F1–Ge1–N4, 94.78(15); F1–Ge1–N1, 90.70(14); N1–Ge1–N4, 74.90(11); N1–Ge2–N4, 81.64(11).



Scheme 2. Selected resonance structures of 3^+ (Dip = 2,6-diisopropylphenyl).

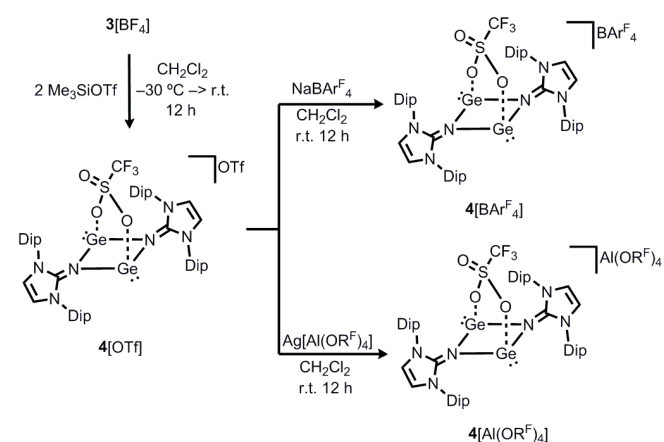


Scheme 3. Conversion of **VIII** to the metal complex **IX** as reported by Power (NBD = bicyclo[2.2.1]hepta-2,5-diene).^[21]

In order to shed light on the validity of the suggested canonical forms theoretical calculations for 3^+ were carried out at the B3LYP level.¹⁸ The MBOs (Mayer Bond Order) of the Ge1–N_{imine} bonds were both calculated to be 0.55 and this value is significantly smaller than the corresponding one of the bis(imino)germylene **VI** (1.12),¹⁸ and even reduced relative to the germyliumylidene cation in **V** (0.68),^{12,18} which underlines the high dative bond character of the Ge1–N_{imine} interactions. In comparison, we determined MBOs of 0.89 for the Ge2–N_{imine} bonds in 3^+ . In accordance with our structural discussion these data verify the germylene-germyliumylidene formulation **A1**. In line with the expectation the MBO of the C_{NHC}–N_{imine} bond (1.32) in 3^+ is comparable to that of **V** (1.24). In addition, we performed NRT (Natural Resonance Theory) analysis in order to gain deeper insight into the nature of the structure of 3^+ . Evaluation of the relative contributions of all important canonical forms for compound 3^+ elucidates that the germylene-germyliumylidene formulation **A1** is dominant (53.7%) which is significantly larger than the resonance form **A2** (8.9%). Additionally, 3^+ possesses significant imidazolium cation character (**A3**, 27.6%). Interestingly, the canonical form **A4**, in which formal positive charge is located at both imidazolium rings with a fluoride anion coordinated to Ge1, has a non-negligible role in the description of 3^+ (9.8%, Scheme 2). The HOMO for 3^+ is mainly the antisymmetric combination of the two lone pairs of the Ge centers (Figure S30).¹⁸ The LUMO for 3^+ is essentially the

vacant p-type atomic orbital on the Ge(II) atom (Ge2) which supports **2** as an intermediate during the formation of 3^+ .¹⁸

With the intention to synthesize a conceivable dicationic [GeNIPr]₂²⁺ species, referred to as bis(germyliumylidene), we converted **3**[BF₄] with two equivalents of Me₃SiOTf as a fluoride scavenger. This resulted in the formation of the triflate salt **4**[OTf] in (Scheme 4). At ambient temperature no decomposition was detected in the solid state, even after storage for weeks under an inert atmosphere. A CD₃CN solution of **4**[OTf] is stable at temperatures up to 60 °C. Unfortunately, X-ray diffraction-quality crystals of **4**[OTf] could not be obtained. The salt **4**[OTf] was converted to **4**[BARF₄] by anion exchange with Na[BARF₄]. It is of note that the dicationic complex [GeNIPr]₂[BARF₄]₂ was not generated by treatment with an excess amount of Na[BARF₄].¹⁸ Single crystals of **4**[BARF₄] suitable for X-ray diffraction analysis were retrieved from a CH₂Cl₂ solution at –30 °C. Similarly, the reaction of **4**[OTf] with the silver salt of the perfluorinated aluminate anion, [Al(OR^F)₄][–] affords the aluminate salt **4**[Al(OR^F)₄]. This reactivity between **4**[OTf] and Ag[Al(OR^F)₄] is contrasted by the treatment of amido-substituted chlorogermylene with Ag[Al(OR^F)₄][–], in which chlorogermylene-silver complex was observed. The Ge₂N₂ germacycle unit possesses the same structure in **4**[BARF₄] and **4**[Al(OR^F)₄]. Therefore, only the structure of the cation of **4**[BARF₄] is depicted in Figure 3. The structural features of **4**[Al(OR^F)₄] are reported in the Supporting Information (Figure S29).¹⁸



Scheme 4. Synthesis of bis(triflate) **4**[OTf] and its conversion to the borate salt **4**[BARF₄], as well as the perfluoroalkoxyalenate **4**[Al(OR^F)₄] (Dip = 2,6-diisopropylphenyl, Ar^F = 3,5-(CF₃)₂-C₆H₃, R^F = C(CF₃)₃).

The molecular structure revealed that, akin to 3^+ , the Ge₂N₂ ring in 4^+ is distorted from square planarity to rhombic geometry. The distances between the Ge- and N_{imine} atoms range from 1.949(2) Å to 1.960(2) Å, which is longer than that of the neutral bis(imino)germylene **VI** (1.8194(15) Å).¹⁵ This emphasizes the partial dative-bond character for the germanium–nitrogen interactions in 4^+ . The C_{NHC}–N_{imine} bonds (1.329(4) Å, 1.335(4) Å) are elongated as compared to those of neutral iminogermynes (1.296(3) Å, 1.273(2) Å),^{14,15} but fall well inside the range of those of the cationic compounds **V**¹⁴ and 3^+ (1.32–1.34 Å), suggesting the delocalization of positive charge into the imidazole ring. Interestingly, the triflyl group in

$4[\text{BAR}^{\text{F}}_4]$ bridges the two germanium centers with the formation of two μ_1^1 type coordinative interactions between the metals and two oxygen atoms. The Ge–O_{triflate} distances (2.250(2) Å, 2.269(2) Å) exceed the scope of typical Ge–O bond lengths (1.75–1.85 Å)²² and fall within the range of Ge–O_{triflate} distances (1.91–2.58 Å),²³ demonstrating the bidentate coordination mode of the triflate ligand. A related structural motif has been reported for cyclic bis(triflate)dibismadiazane [(TfO)Bi(NTer)]₂ (Ter = 2,6-bis(2,4,6-trimethylphenyl)phenyl).²⁴

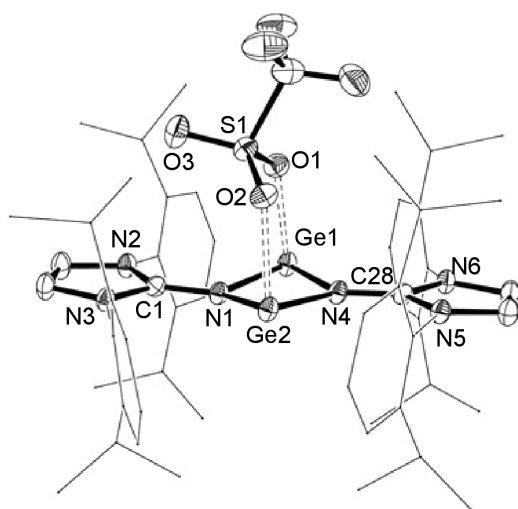
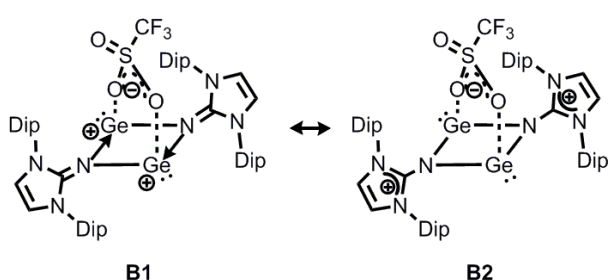


Figure 3. ORTEP representation of the molecular structure of the cation in $4[\text{BAR}^{\text{F}}_4]$ in the solid state. Thermal ellipsoids are at the 40% probability level. Dip groups are depicted as stick models. Hydrogen atoms are omitted for clarity. Selected bond lengths (Å) and bond angles (deg): Ge1–N4, 1.956(2); Ge1–N1, 1.959(2); Ge1–O1, 2.250(2); Ge2–N4, 1.949(2); Ge2–N1, 1.960(2); Ge2–O2, 2.269(2); N1–C1, 1.329(4); N2–C1, 1.363(4); N3–C1, 1.367(4); N4–C28, 1.335(4); N5–C28, 1.363(4); N6–C28, 1.362(4); N1–Ge1–N4, 78.18(10); N1–Ge1–O1, 87.53(9); N4–Ge1–O1, 90.10(9); N1–Ge2–N4, 78.34(10); N1–Ge2–O2, 88.22(9); N4–Ge2–O2, 88.60(9); C1–N1–Ge1, 128.0(2); C1–N1–Ge2, 128.5(2); Ge1–N1–Ge2, 100.80(10); C28–N4–Ge2, 129.3(2); C28–N4–Ge1, 129.1(2); Ge1–N4–Ge2 101.31(10).



Scheme 5. Selected resonance structures of 4^+ (Dip = 2,6-diisopropylphenyl).

In order to gain further insight into the electronic properties of the germanium(II) cation 4^+ , quantum chemical calculations were carried out. The calculated MBOs for the Ge–N_{imine} bonds in 4^+ amount to 0.74 each, which is significantly smaller than that of **VI** (1.12) though somewhat larger than the germanium-imino dative bond of **V** (0.68). Moreover, the bonding characteristics of 4^+ were analyzed by means of NRT. The study shows that the dominant resonance form is **B1** (71.6 %), in which a positive

charge resides on each Ge(II) center and a coordinated triflyl moiety bears a negative charge (Scheme 5).

The resonance structure **B2** has also considerable weight (28.4%) and represents the imidazolium cation character of 4^+ . For comparison, we calculated the optimized structure of the hypothetical dication $[(\text{GeNIPr})_2]^{2+}$ by removing the bridging triflate anion from 4^+ . We found that the structural parameters of $[(\text{GeNIPr})_2]^{2+}$ are in good agreement with those of the triflate-germyliumylidene 4^+ , which indicates that the bridging triflate has a minor effect on the geometry of the dicationic moiety. However, the presumed bis(germyliumylidene) character for $[(\text{GeNIPr})_2]^{2+}$ is mitigated by its NRT analysis for which the contribution of imidazolium cation resonance structures as represented by **B2** has higher weight (39.1%) in comparison with that in 4^+ (28.4%). This is probably due to destabilization of the hypothetical bis(germyliumylidene) dication by the electronic repulsion between the two Ge(II) centers.¹⁸ This result implies that the coordinated triflate anion is crucial for the stabilization of the bis(germyliumylidene) form **B1**. The LUMO and the LUMO+1 for 4^+ exhibit vacant p-orbitals on the Ge(II) centers (Figure S31).¹⁸ The HOMO corresponds to the π -orbitals of the imino ligands while HOMO–1 shows mainly the antisymmetric combination of the lone pair orbitals on the germanium centers which indicates consistent picture with the NRT analysis.

In summary, we report the syntheses of the imino-stabilized bis(germanium) monocation $3[\text{BF}_4]$ and its derivative $3[\text{BAR}^{\text{F}}_4]$ obtained via anion exchange. The cation 3^+ marks a unique germylene-germyliumylidene species which features a two-coordinate germylene and three-coordinated germyliumylidene functionality incorporated into a four-membered digermametallacycle. Additionally, the substitution of fluoride in $3[\text{BF}_4]$ by triflate yields $4[\text{OTf}]$, which can be converted to $4[\text{BAR}^{\text{F}}_4]$ and $4[\text{Al}(\text{OR}^{\text{F}})_4]$ with one triflyl group coordinated to the germanium centers in a bridging fashion, as well as a non-coordinated counteranion. Computational study of 4^+ show that the $[(\text{GeNIPr})_2]$ moiety possesses properties of a dication which suggests considerable bis(germyliumylidene) character for this ionic compound.

Acknowledgements

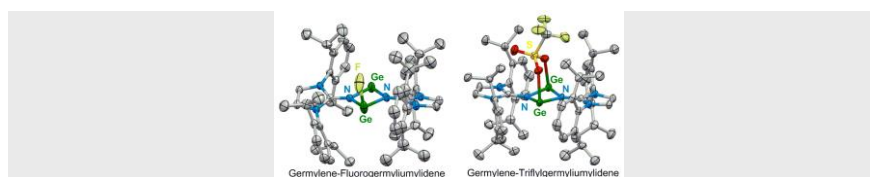
We are exceptionally grateful to the Alexander von Humboldt Foundation (Sofja Kovalevskaja Program) and the European Research Council (ERC Staring Grant 637394 “SILION”) for financial support. We thank Paula Nixdorf for collecting X-ray diffraction data. T. S. is thankful for the support of The New Széchenyi Plan TAMOP-4.2.2/B-10/1-2010-0009.

Keywords: germanium • germylene • germyliumylidene • dication • imine

- [1] For review on germyliumylidenes see: V. S. V. S. N. Swamy, S. Pal, S. Khan, S. S. Sen, *Dalton Trans.* **2015**, *44*, 12903 and references cited therein.
- [2] P. Jutzi, F. Kohl, P. Hofmann, C. Krüger, Y. Tsay, *Chem. Ber.* **1980**, *113*, 757.

- [3] a) H. V. R. Dias, Z. Wang, *J. Am. Chem. Soc.* **1997**, *119*, 4650. b) M. Stender, A. D. Phillips, P. P. Power, *Inorg. Chem.* **2001**, *40*, 5314; c) A. Schäfer, W. Saak, D. Haase, T. Müller, *Chem. Eur. J.* **2009**, *15*, 3945; d) F. Cheng, J. M. Dyke, F. Ferrante, A. L. Hector, W. Levason, G. Reid, M. Webster, W. Zhang, *Dalton Trans.* **2010**, 39, 847; e) A. P. Singh, H. W. Roesky, E. Carl, D. Stalke, J.-P. Demers, A. Lange, *J. Am. Chem. Soc.* **2012**, *134*, 4998; f) Y. Xiong, S. Yao, S. Inoue, A. Berkefeld, M. Driess, *Chem. Commun.* **2012**, 48, 12198; g) J. Li, C. Schenk, F. Winter, H. Scherer, N. Trapp, A. Higelin, S. Keller, R. Pöttgen, I. Krossing, C. Jones, *Angew. Chem. Int. Ed.* **2012**, *51*, 9557; *Angew. Chem.* **2012**, *124*, 9695; h) Y. Xiong, S. Yao, G. Tan, S. Inoue, M. Driess, *J. Am. Chem. Soc.* **2013**, *135*, 5004; i) M. Bouska, L. Dostál, A. Růžicka, R. Jambor, *Organometallics* **2013**, *32*, 1995; j) S. Khan, G. Gopakumar, W. Thiel, M. Alcarazo, *Angew. Chem. Int. Ed.* **2013**, *52*, 5644; k) B. Su, R. Ganguly, Y. Li, R. Kinjo, *Chem. Commun.* **2016**, 52, 613; l) A. Rit, R. Tirfoin, S. Aldridge, *Angew. Chem. Int. Ed.* **2016**, *55*, 378; *Angew. Chem.* **2016**, *128*, 386.
- [4] a) P. A. Rugar, V. N. Staroverov, P. J. Ragogna, K. M. Baines, *J. Am. Chem. Soc.* **2007**, *129*, 15138; b) P. M. Rugar, V. N. Staroverov, K. M. Baines, *Science* **2008**, *322*, 1360; c) P. A. Rugar, R. Bandyopadhyay, B. F. T. Cooper, M. R. Stinchcombe, P. J. Ragogna, C. L. B. MacDonald, K. M. Baines, *Angew. Chem. Int. Ed.* **2009**, *48*, 5155; *Angew. Chem.* **2009**, *121*, 5257; d) F. Cheng, A. L. Hector, W. Levason, G. Reid, M. Webster, W. Zhang, *Angew. Chem. Int. Ed.* **2009**, *48*, 5152; *Angew. Chem.* **2009**, *121*, 5254; e) M. J. Ward, P. A. Rugar, M.W. Murphy, Y.-M. Yiu, K. M. Baines, T. K. Sham, *Chem. Commun.* **2010**, 46, 7016; For dicationic complexes of tin(II) or silicon(II) see: f) R. Bandyopadhyay, B. F. T. Cooper, A. J. Rossini, R. W. Schurko, C. L. B. Macdonald, *J. Organomet. Chem.* **2010**, *695*, 1012; g) A. C. Filippou, Y. N. Lebedev, O. Chernov, M. Straßmann, G. Schnakenburg, *Angew. Chem. Int. Ed.* **2013**, *52*, 6974; *Angew. Chem.* **2013**, *125*, 7112.
- [5] N. Kano, H. Miyake, K. Sasaki, T. Kawashima, N. Mizorogi, S. Nagase, *Nat. Chem.* **2010**, *2*, 112.
- [6] a) K. Inomata, T. Watanabe, H. Tobita, *J. Am. Chem. Soc.* **2014**, *136*, 14341; b) K. Inomata, T. Watanabe, Y. Miyazaki, H. Tobita, *J. Am. Chem. Soc.* **2015**, *137*, 11935.
- [7] S. P. Green, C. Jones, P. C. Junk, K.-A. Lippert, A. Stasch, *Chem. Commun.* **2006**, 3978.
- [8] a) S. Nagendran, S. S. Sen, H. W. Roesky, D. Koley, H. Grubmüller, A. Pal, R. Herbst-Irmer, *Organometallics* **2008**, *27*, 5459; b) W. Wang, S. Inoue, S. Yao, M. Driess, *Chem. Commun.* **2009**, 2661; c) W.-P. Leung, W.-K. Chiu, K.-H. Chong, T. C. W. Mak, *Chem. Commun.* **2009**, 6822; d) C. Jones, S. J. Bonyhady, N. Holzmann, G. Frenking, A. Stasch, *Inorg. Chem.* **2011**, *50*, 12315; e) W.-P. Leung, W.-K. Chiu, T. C. W. Mak, *Organometallics* **2014**, *33*, 225.
- [9] A. V. Zabula, F. E. Hahn, T. Pape, A. Hepp, *Organometallics* **2007**, *26*, 1972.
- [10] a) F. E. Hahn, A. V. Zabula, T. Pape, A. Hepp, *Z. Anorg. Allg. Chem.* **2008**, *634*, 2397; b) A. Brück, D. Gallego, W. Wang, E. Irran, M. Driess, J. F. Hartwig, *Angew. Chem. Int. Ed.* **2012**, *51*, 11478; *Angew. Chem.* **2012**, *124*, 11645; c) W. Wang, S. Inoue, S. Enthaler, M. Driess, *Angew. Chem. Int. Ed.* **2012**, *51*, 6167; *Angew. Chem.* **2012**, *124*, 6271; d) D. Gallego, A. Brück, E. Irran, F. Meier, M. Kaupp, M. Driess, J. F. Hartwig, *J. Am. Chem. Soc.* **2013**, *135*, 15617; e) D. Gallego, S. Inoue, B. Blom, M. Driess, *Organometallics* **2014**, *33*, 6885; f) L. Álvarez-Rodríguez, J. A. Cabeza, P. García-Álvarez, D. Polo, *Coord. Chem. Rev.* **2015**, *300*, 1.
- [11] a) M. Veith, *Angew. Chem. Int. Ed.* **1975**, *14*, 263; b) M. Veith, M. Grosser, *Z. Naturforsch. B* **1982**, *37*, 1375; c) M. Veith, *Angew. Chem. Int. Ed.* **1987**, *26*, 1.
- [12] P. Steiniger, G. Bendt, D. Bläser, C. Wölper, S. Schulz, *Chem. Commun.* **2014**, 50, 15461.
- [13] T. Ochiai, D. Franz, E. Irran, S. Inoue, *Chem. Eur. J.* **2015**, *21*, 6704.
- [14] T. Ochiai, D. Franz, X.-N. Wu, S. Inoue, *Dalton Trans.* **2015**, 44, 10952.
- [15] M. W. Lui, C. Merten, M. J. Ferguson, R. McDonald, Y. Xu, E. Rivard, *Inorg. Chem.* **2015**, *54*, 2040.
- [16] T. Ochiai, D. Franz, X.-N. Wu, E. Irran, S. Inoue, *Angew. Chem. Int. Ed.* **2016**, *55*, 6983.
- [17] R. Kinjo, B. Donnadiu, G. Bertrand, *Angew. Chem. Int. Ed.* **2010**, *49*, 5930; *Angew. Chem.* **2010**, *122*, 6066.
- [18] For the experimental procedures, spectral data and crystal data of $3[\text{BF}_4]$, $3[\text{BA}^{\text{F}}_4]$, $4[\text{OTf}]$, $4[\text{BA}^{\text{F}}_4]$ and $4[\text{Al}(\text{OR}^{\text{F}})_4]$ and details of the theoretical studies, see the Supporting Information.
- [19] a) A. Jana, P. P. Samuel, H. W. Roesky, C. Schulzke, *J. Fluorine Chem.* **2010**, *131*, 1096. b) Y. Ding, Q. Ma, I. Usón, H. W. Roesky, M. Noltemeyer, H.-G. Schmidt, *J. Am. Chem. Soc.* **2002**, *124*, 8542. c) R. Tacke, J. Heermann, M. Pülm, *Z. Naturforsch.* **1998**, *53 b*, 535. d) Y. Ding, Q. Ma, H. W. Roesky, I. Usón, M. Noltemeyer, H.-G. Schmidt, *Dalton Trans.* **2003**, 1094. e) E. Lukevics, S. Belyakov, P. Arsenyan, J. Popelis, *J. Organomet. Chem.* **1997**, *549*, 163.
- [20] F. Breher, H. Rügger, *Angew. Chem. Int. Ed.* **2005**, *44*, 473; *Angew. Chem.* **2005**, *117*, 477.
- [21] F. Lips, J. D. Queen, J. C. Fettinger, P. P. Power, *Chem. Commun.* **2014**, 50, 5561.
- [22] K. M. Baines, W. G. Stibbs, *Coord. Chem. Rev.* **1995**, *145*, 157 and references cited therein.
- [23] The search was carried out through the Cambridge Structural Database (CSD) version 5.36 (November 2014).
- [24] M. Lehmann, A. Schulz, A. Villinger, *Angew. Chem. Int. Ed.* **2012**, *51*, 8087; *Angew. Chem.* **2012**, *124*, 8211.

COMMUNICATION



*Tatsumi Ochiai, Tibor Szilvási, Daniel Franz, Elisabeth Irran, Shigeyoshi Inoue**

Page No. – Page No.

Isolation and Structure of Germylene–Germyliumylidenes stabilized by N-Heterocyclic Imine

Double charge: A monocationic four-membered germacycle is prepared by fluorination of an amino(imino)germylene followed by fluoride abstraction. The nature of the bonding situation is analyzed computationally and indicates that the germylene-stabilized germyliumylidene character is dominant. Substitution of germylene-germyliumylidene with Me_3SiOTf affords a unique triflyl-substituted germylene-germyliumylidene with pronounced dicationic bis(germyliumylidene) character.

Author Manuscript

Supporting Information for the Communication

**Isolation and Structure of Germylene–
Germyliumylidenes stabilized by N-Heterocyclic Imine**

Tatsumi Ochiai,^[a] Tibor Szilvaši,^[b] Daniel Franz,^[c] Elisabeth Irran,^[a] and
Shigeyoshi Inoue*^[a,c]

^a Institut für Chemie, Technische Universität Berlin, Straße des 17. Juni 135, 10623 Berlin (Germany)

^b Department of Inorganic and Analytical Chemistry, Budapest University of Technology and Economics,
Szent Gellért tér 4, 1111 Budapest (Hungary)

^c Department of Chemistry, Catalysis Research Center and Institute of Silicon Chemistry, Technische
Universität München, Lichtenbergstraße 4, 85748 Garching (Germany)

Author Manuscript

Contents

1.) Experimental Details	3
2.) Crystallographic Data of 3 [BF ₄], 3 [BAr ^F ₄], 4 [BAr ^F ₄] and 4 [Al(OR ^F) ₄]	19
3.) Details to the DFT Calculations	24
4.) Supplementary References	60

1.) Experimental Details

General considerations: All experiments and manipulations were conducted under dry oxygen-free nitrogen using standard Schlenk techniques or in an MBraun glovebox workstation containing an atmosphere of purified nitrogen. Solvents were dried by standard methods. NMR solvents were degassed by multiple freeze-pump-thaw cycles and stored over molecular sieves (3 Å). Reagents were purchased from commercial suppliers and processed as received if not stated otherwise. The starting material amino(imino)germylene **1** was prepared according to the reported procedure.^[S1] ¹H-, ¹¹B-, ¹³C{¹H}-, and ¹⁹F- spectra were recorded on a Bruker Avance II 200 MHz or 400 MHz spectrometer and referenced to residual solvent signals as internal standards (¹H and ¹³C) or an external standard (Et₂O•BF₃ for ¹¹B, and CFCI₃ for ¹⁹F). Values for the chemical shift (δ) are given in parts per million. Abbreviations: s = singlet; d = doublet; t = triplet; sept = septet; br = broad; n.r. = not resolved; n.o. = not observed; Dip = 2,6-diisopropylphenyl; Ar^F = 3,5-(CF₃)₂-C₆H₃; OR^F = OC(CF₃)₃. Elemental analyses and ESI-HRMS were carried out by the microanalytical laboratory and the MS-Service of the Institut für Chemie, Technische Universität Berlin, Germany, respectively.

Synthetic Procedure and Analytical Data for 3[BF₄]

To a stirring mixture of amino(imino)germylene **1** (1.17 g, 1.84 mmol) in toluene (10 ml) was added BF₃•Et₂O (0.46 ml, 3.72 mmol) via syringe at -78 °C. The reaction mixture was stirred for 12 h while allowed to slowly warm to room temperature. The solvent was removed under vacuum and the residue washed with Et₂O (5 ml) to give 3[BF₄] as a yellow solid (1.67 g, 86%). Recrystallization from THF (3 ml) afforded 3[BF₄] in the form of colorless crystals (854 mg, 44%). The batch contained single crystals suitable for X-ray diffraction analysis.

¹H NMR (200.1 MHz, THF-*d*₈): δ = 1.12 (d, ³J_{HH} = 7 Hz, 24H, CH(CH₃)₂), 1.16 (d, ³J_{HH} = 7 Hz, 24H, CH(CH₃)₂), 2.56 (sept, ³J_{HH} = 7 Hz, 8H, CH(CH₃)₂), 7.13 (s, 4H, NCH), 7.24 (d, ³J_{HH} = 8 Hz, 8H, Ar-H), 7.48 (t, ³J_{HH} = 8 Hz, 4H, Ar-H). ¹³C{¹H} NMR (100.6 MHz, THF-*d*₈): δ = 23.1 (CH(CH₃)₂), 25.1 (CH(CH₃)₂), 29.8 (CH(CH₃)₂), 119.6 (NCH), 126.5 (Ar-C), 132.4 (Ar-C), 132.7 (Ar-C), 147.4 (Ar-C), 151.4 (NCN). ¹¹B NMR (64.2 MHz, THF-*d*₈): δ = -2.9 (n. r.). ¹⁹F NMR (188.3 MHz, THF-*d*₈): δ = -153.9 (n. r., BF₄), -63.1 (GeF). ESI-HRMS: *m/z* (positive ion mode): 969.4253 (calc. 969.4230 for [M - BF₄]⁺). ESI-HRMS: *m/z* (negative ion mode): 87.0033 (calc. 87.0024 for [BF₄]⁻). M.p. at 291-294 °C (dec.).

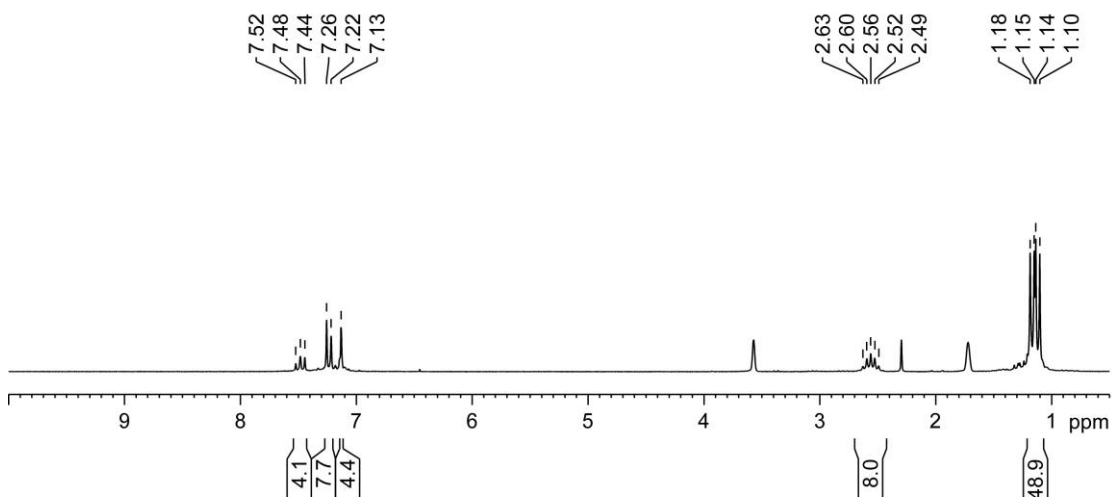


Figure S1. ¹H NMR spectrum (200.1 MHz, THF-*d*₈) of 3[BF₄].

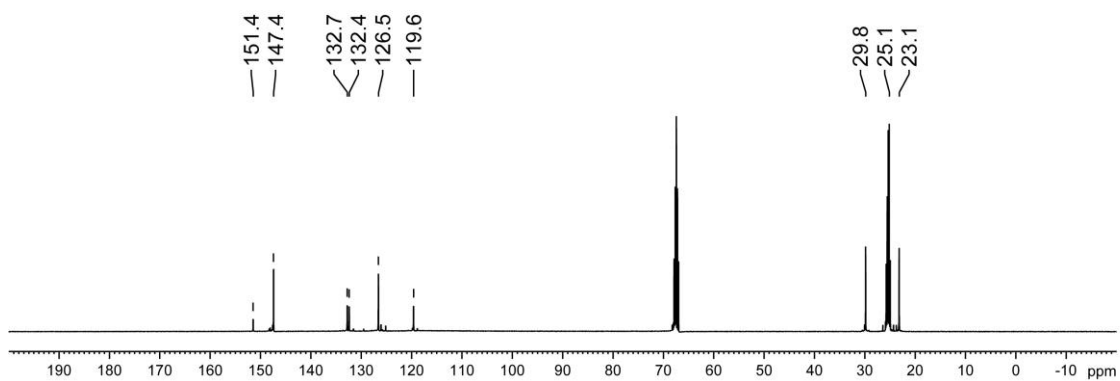


Figure S2. $^{13}\text{C}\{^1\text{H}\}$ NMR spectrum (100.6 MHz, $\text{THF-}d_8$) of $3[\text{BF}_4]$.

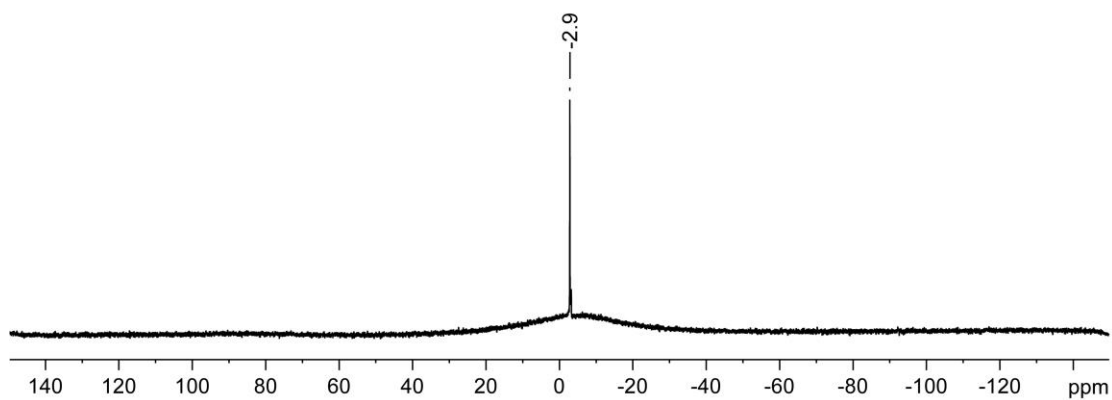


Figure S3. ^{11}B NMR spectrum (64.2 MHz, $\text{THF-}d_8$) of $3[\text{BF}_4]$.

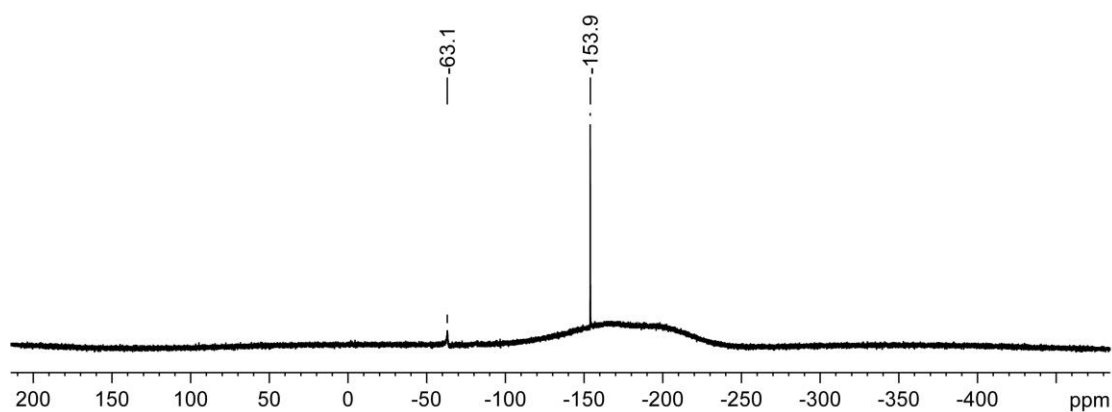


Figure S4. ^{19}F NMR spectrum (188.3 MHz, $\text{THF-}d_8$) of $3[\text{BF}_4]$.

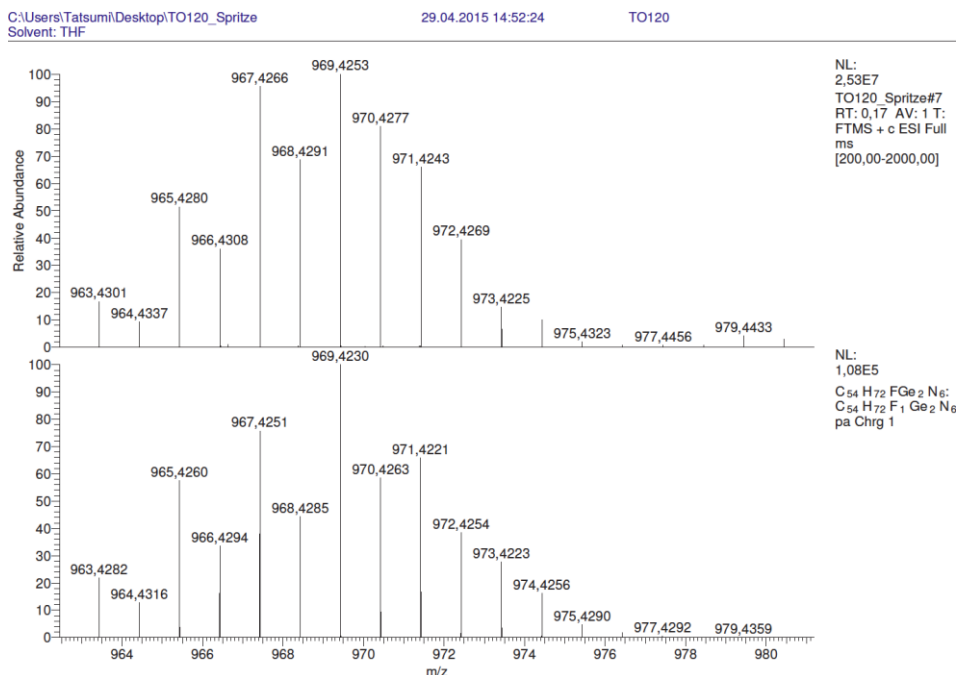


Figure S5. Signal of $[M - BF_4]^+$ as observed in the ESI-HRMS (positive ion mode) analysis of $3[BF_4]$. Top (expt.), bottom (calc.).

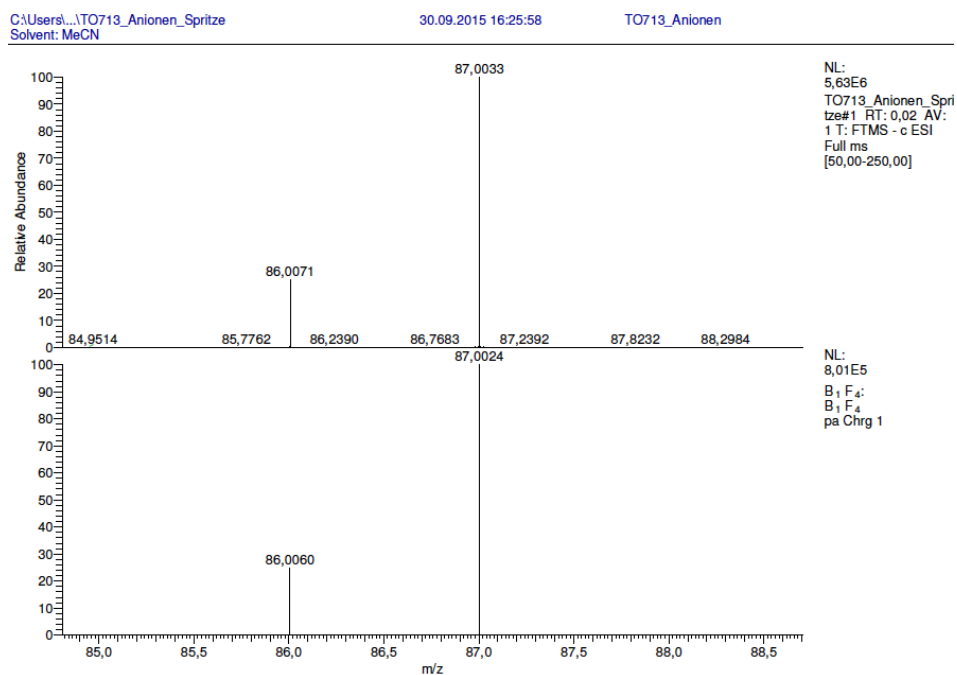


Figure S6. Signal of $[BF_4]^-$ as observed in the ESI-HRMS (negative ion mode) analysis of $3[BF_4]$. Top (expt.), bottom (calc.).

Synthetic Procedure and Analytical Data for 3[BAr^F₄]

A Schlenk tube equipped with a PTFE-coated magnetic stirring bar was charged with 3[BF₄] (239 mg, 0.226 mmol) and Na[BAr^F₄] (401 mg, 0.727 mmol). CH₃CN (10 ml) was transferred to the reaction vessel by cannula at -30 °C and the resulting mixture was stirred for 12 h while allowed to slowly warm to room temperature. The volatiles were removed under reduced pressure and the residue was recrystallized from CH₃CN (5 ml) at -30 °C to afford 3[BAr^F₄] as colorless crystals (211 mg, 51%). The batch contained crystals suitable for single crystal X-ray diffraction analysis.

¹H NMR (400.1 MHz, CD₃CN): δ = 1.09 (d, ³J_{HH} = 6 Hz, 24H, CH(CH₃)₂), 1.13 (d, ³J_{HH} = 6 Hz, 24H, CH(CH₃)₂), 2.49 (sept, ³J_{HH} = 6 Hz, 8H, CH(CH₃)₂), 6.94 (s, 4H, NCH), 7.21 (d, ³J_{HH} = 8 Hz, 8H, Ar-H), 7.43 (t, ³J_{HH} = 8 Hz, 4H, Ar-H), 7.67 (br, 4H, Ar^F-H_{para}), 7.70 (br, 8H, Ar^F-H_{ortho}). ¹³C{¹H} NMR (100.6 MHz, CD₃CN): δ = 22.9 (CH(CH₃)₂), 25.0 (CH(CH₃)₂), 29.8 (CH(CH₃)₂), 118.7 (m, Ar^F-C_{para}), 119.3 (NCH), 125.5 (q, ¹J_{CF} = 273 Hz, CF₃), 126.7 (Ar-C), 129.8 (q, ²J_{CF} = 31 Hz, Ar^F-C_{meta}), 132.1 (Ar-C), 132.8 (Ar-C), 135.7 (br, Ar^F-C_{ortho}), 147.6 (Ar-C), 151.6 (NCN), 162.6 (q, ¹J_{CB} = 49 Hz, Ar^F-C_{ipso}). ¹¹B NMR (64.2 MHz, CD₃CN): δ = -6.7. ¹⁹F NMR (188.3 MHz, CD₃CN): δ = -63.3 (CF₃), -62.8 (GeF). Elemental analysis calc. (%) for C₈₆H₈₄BF₂₅Ge₂N₆: C 56.36, H 4.62, N 4.59; found: C 56.67, H 4.92, N 4.51. M.p. at 274-276 °C (dec.).

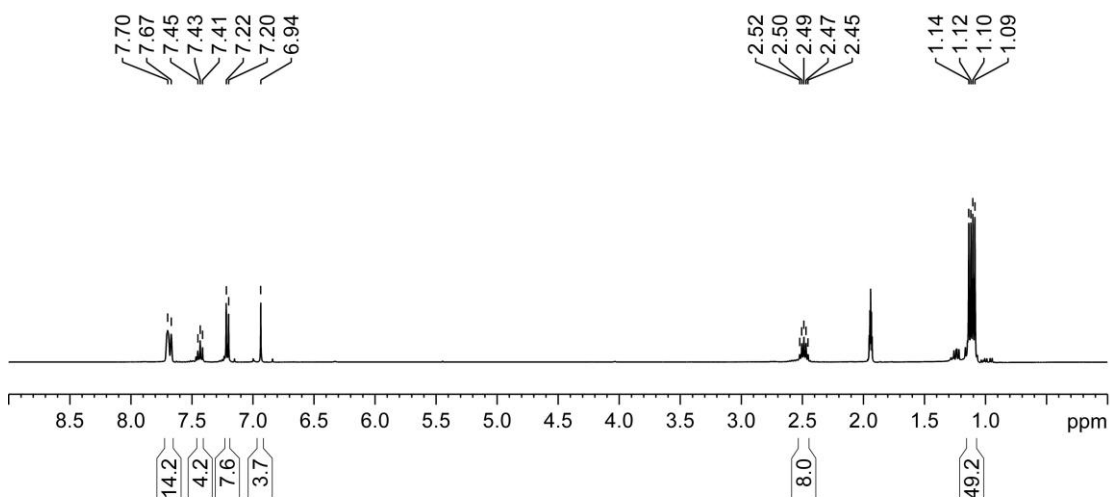


Figure S7. ¹H NMR spectrum (400.1 MHz, CD₃CN) of 3[BAr^F₄].

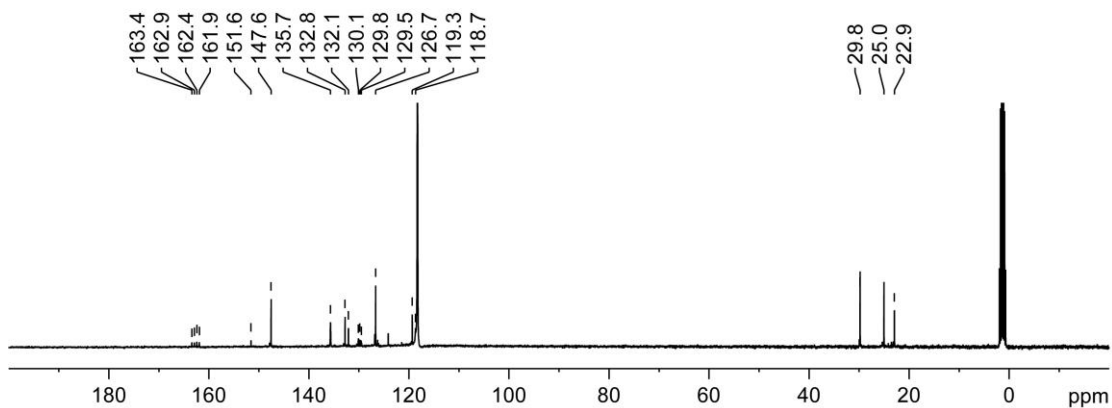


Figure S8. $^{13}\text{C}\{^1\text{H}\}$ NMR spectrum (100.6 MHz, CD_3CN) of $3[\text{BAr}^{\text{F}}_4]$.

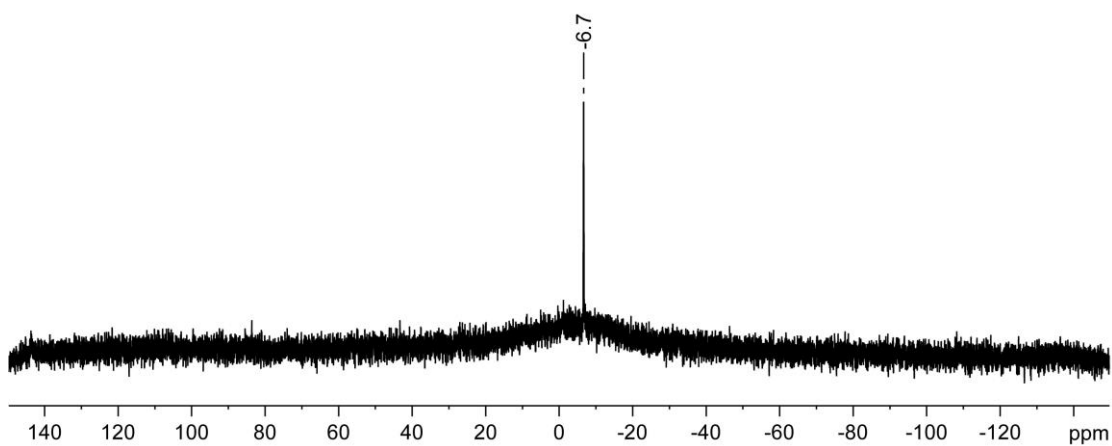


Figure S9. ^{11}B NMR spectrum (64.2 MHz, CD_3CN) of $3[\text{BAr}^{\text{F}}_4]$.

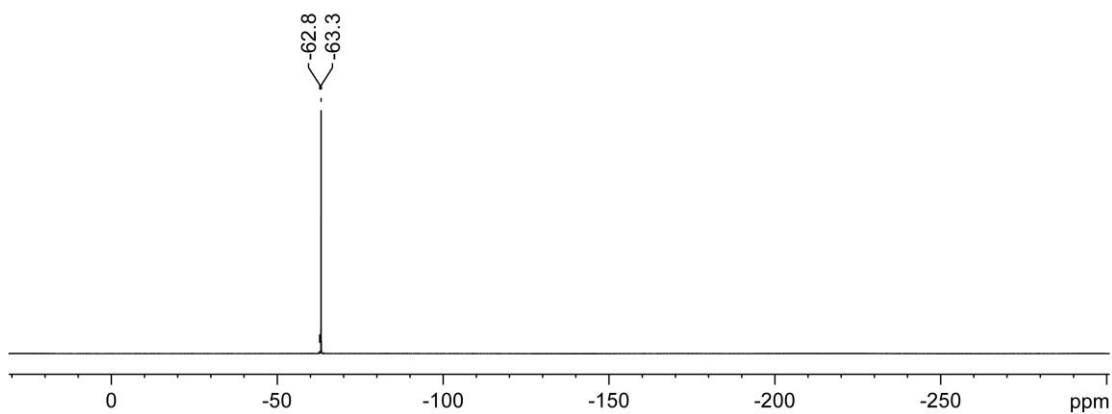


Figure S10. ^{19}F NMR spectrum (188.3 MHz, CD_3CN) of $3[\text{BAr}^{\text{F}}_4]$.

Synthetic Procedure and Analytical Data for 4[OTf]

Me₃SiOTf (0.2 ml, 1.10 mmol) was added to a stirring mixture of **3**[BF₄] (525 mg, 0.497 mmol) in CH₂Cl₂ (10 ml) via syringe at -78 °C. The reaction mixture was stirred for 12 h while allowed to slowly warm to room temperature. The solvent was removed under vacuum. The residue was recrystallized from CH₂Cl₂ (5 ml) at -30 °C to give **4**[OTf] as colorless crystals (409 mg, 66%). The batch contained single crystals suitable for X-ray diffraction analysis.

¹H NMR (200.1 MHz, CD₃CN): δ = 1.08 (d, ³J_{HH} = 8 Hz, 24H, CH(CH₃)₂), 1.19 (d, ³J_{HH} = 8 Hz, 24H, CH(CH₃)₂), 2.58 (sept, ³J_{HH} = 8 Hz, 8H, CH(CH₃)₂), 7.02 (s, 4H, NCH), 7.24 (d, ³J_{HH} = 8 Hz, 8H, Ar-H), 7.46 (t, ³J_{HH} = 8 Hz, 4H, Ar-H). ¹³C{¹H} NMR (100.6 MHz, CD₃CN): δ = 22.8 (CH(CH₃)₂), 25.9 (CH(CH₃)₂), 29.6 (CH(CH₃)₂), 119.9 (NCH), 126.9 (Ar-C), 132.0 (Ar-C), 133.5 (Ar-C), 147.8 (Ar-C), 151.3 (NCN). ¹⁹F NMR (188.3 MHz, CD₃CN): δ = -79.2. ESI-HRMS: *m/z* (positive ion mode): 1099.3773 (calc. 1099.3766 for [M - OTf]⁺). ESI-HRMS: *m/z* (negative ion mode): 148.9519 (calc. 148.9515 for [OTf]⁻). M.p. at 225-228 °C (dec.).

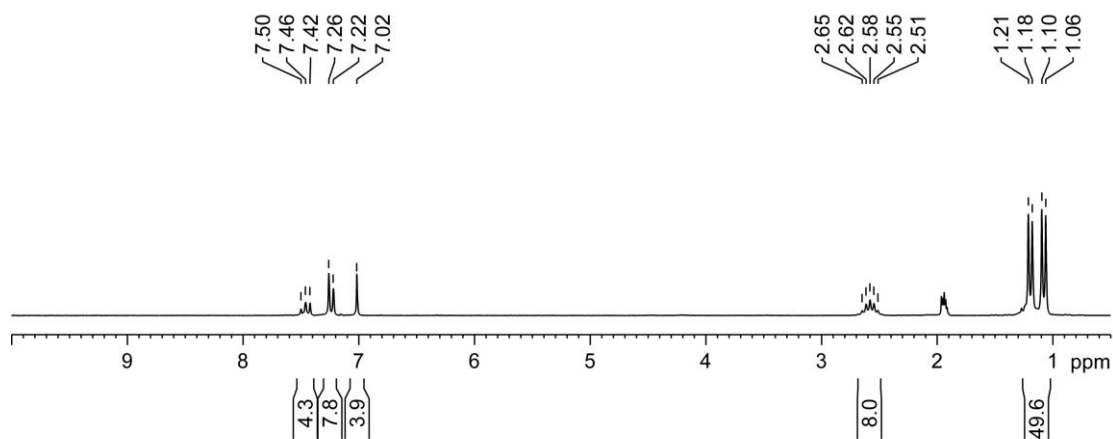


Figure S11. ¹H NMR spectrum (200.1 MHz, CD₃CN) of **4**[OTf].

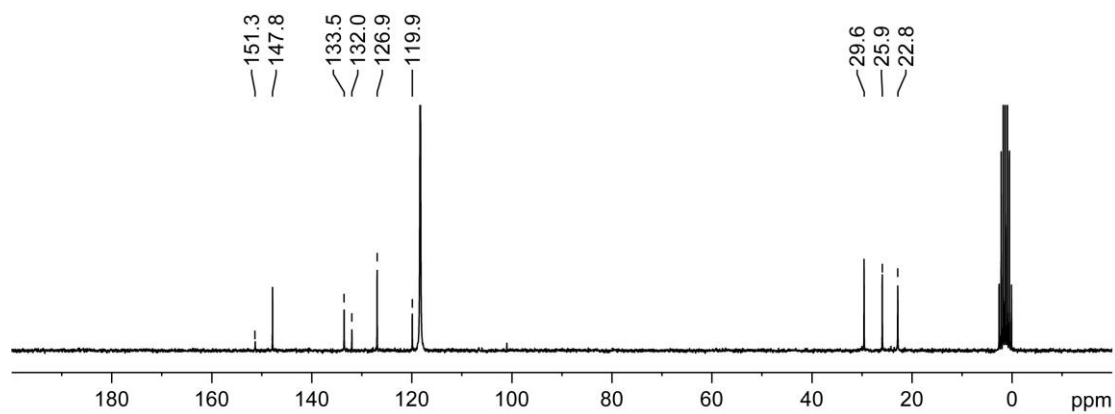


Figure S12. $^{13}\text{C}\{^1\text{H}\}$ NMR spectrum (100.6 MHz, CD_3CN) of 4[OTf]

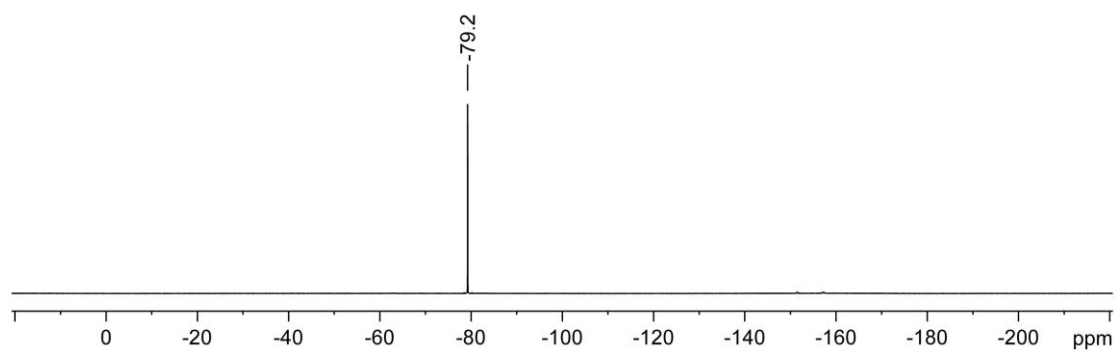


Figure S13. ^{19}F NMR spectrum (188.3 MHz, CD_3CN) of 4[OTf].

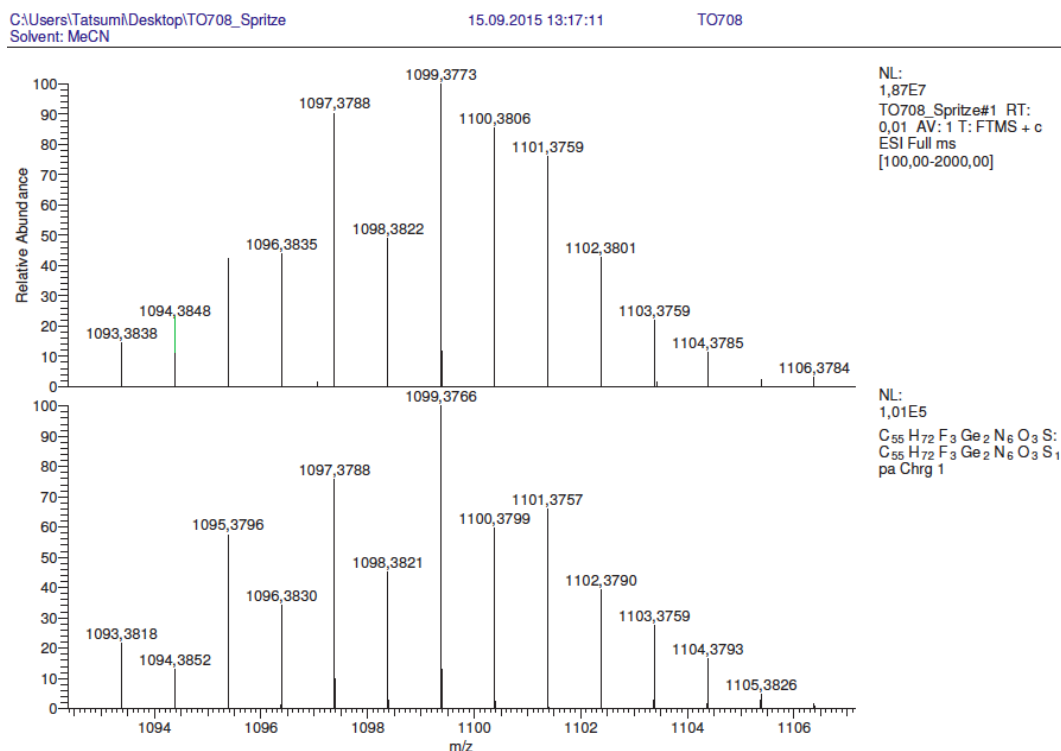


Figure S14. Signal of $[M - OTf]^+$ as observed in the ESI-HRMS (positive ion mode) analysis of **4**[OTf]. Top (expt.), bottom (calc.).

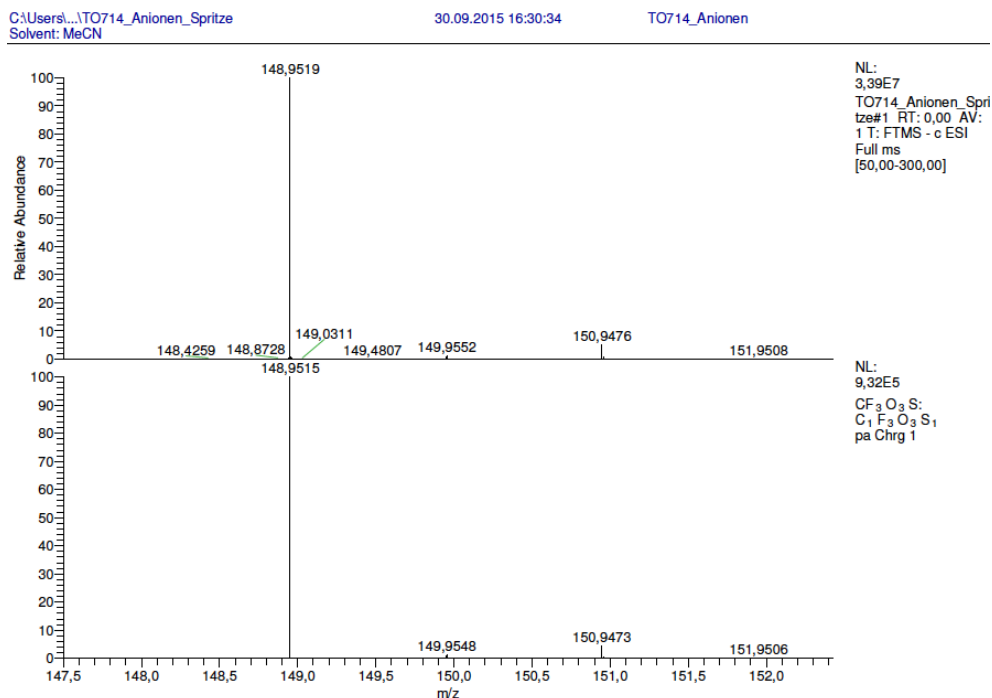


Figure S15. Signal of $[OTf]^-$ as observed in the ESI-HRMS (negative ion mode) analysis of **4**[OTf]. Top (expt.), bottom (calc.).

Synthetic Procedure and Analytical Data for 4[BAr^F₄]

A Schlenk tube equipped with a PTFE-coated magnetic stirring bar was charged with 4[OTf] (222 mg, 0.178 mmol) and Na[BAr^F₄] (315 mg, 0.355 mmol). CH₃CN (10 ml) was transferred to the reaction vessel by cannula at -30 °C and the resulting mixture was stirred for 12 h while allowed to slowly warm to room temperature. The volatiles were removed under reduced pressure and recrystallization of the residue from CH₂Cl₂ at -30 °C afforded 4[BAr^F₄] as colorless crystals (146 mg, 42%). Colorless crystals of 4[BAr^F₄] of suitable quality for X-ray crystallography were obtained from CH₃CN at -30 °C.

¹H NMR (200.1 MHz, CD₂Cl₂): δ = 1.08 (d, ³J_{HH} = 7 Hz, 24H, CH(CH₃)₂), 1.20 (d, ³J_{HH} = 7 Hz, 24H, CH(CH₃)₂), 2.62 (sept, ³J_{HH} = 8 Hz, 8H, CH(CH₃)₂), 6.70 (s, 4H, NCH), 7.18 (d, ³J_{HH} = 8 Hz, 8H, Ar-H), 7.39 (t, ³J_{HH} = 8 Hz, 4H, Ar-H), 7.56 (br, 4H, Ar^F-H_{para}), 7.72 (br, 8H, Ar^F-H_{ortho}). ¹³C{¹H} NMR (100.6 MHz, CD₂Cl₂): δ = 22.6 (CH(CH₃)₂), 26.0 (CH(CH₃)₂), 29.0 (CH(CH₃)₂), 117.9 (n.r., Ar^F-C_{para}), 118.7 (NCH), 125.0 (q, ¹J_{CF} = 273 Hz, CF₃), 126.2 (Ar-C), 129.9 (q, ²J_{CF} = 31 Hz, Ar^F-C_{meta}), 131.3 (Ar-C), 132.7 (Ar-C), 135.2 (br, Ar^F-C_{ortho}), 147.4 (Ar-C), 150.9 (NCN), 162.2 (q, ¹J_{CB} = 50 Hz, Ar^F-C_{ipso}). ¹¹B NMR (64.2 MHz, CD₂Cl₂): δ = -6.6. ¹⁹F NMR (188.3 MHz, CD₂Cl₂): δ =, -79.1 (SO₃CF₃), -62.8 (Ar-CF₃). ESI-HRMS: *m/z* (positive ion mode): 1099.3754 (calc. 1099.3766 for [M - BAr^F₄]⁺). ESI-HRMS: *m/z* (negative ion mode): 863.0640 (calc. 863.0643 for [BAr^F₄]⁻). Elemental analysis calc. (%) for C₈₇H₈₄BF₂₇Ge₂N₆O₃S•2CH₂Cl₂: C 50.13, H 4.16, N 3.94, S 1.50; found: C 50.73, H 4.25, N 3.62, S 1.11. M.p. at 214-216 °C (dec.).

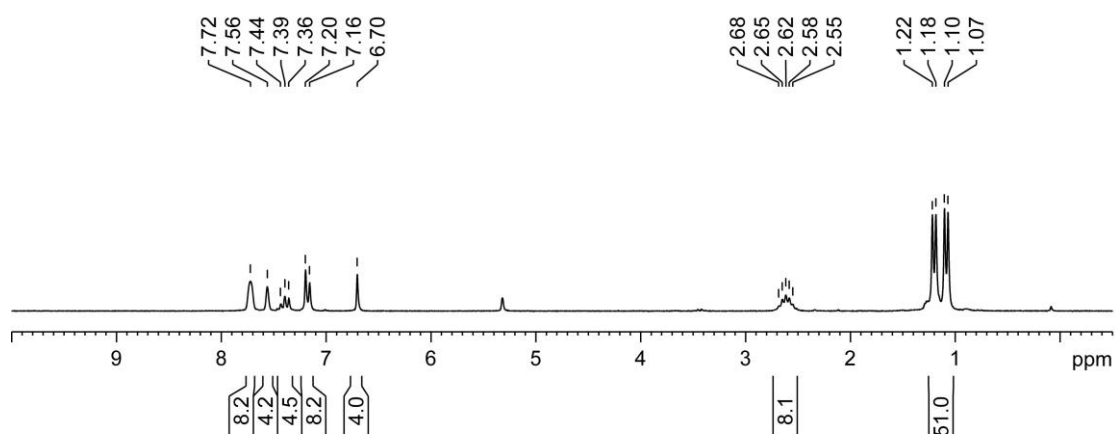


Figure S16. ¹H NMR spectrum (200.1 MHz, CD₂Cl₂) of 4[BAr^F₄].

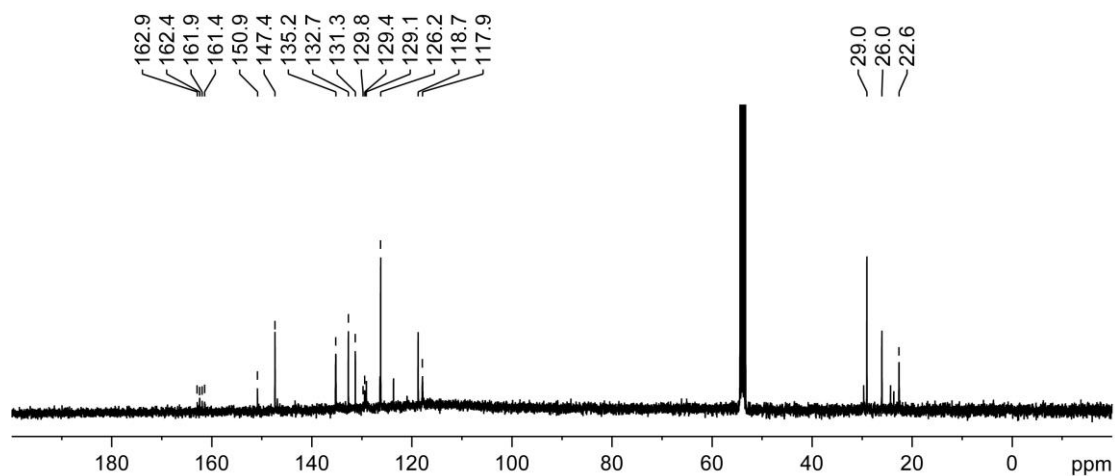


Figure S17. $^{13}\text{C}\{^1\text{H}\}$ NMR spectrum (100.6 MHz, CD_2Cl_2) of $4[\text{BAr}^{\text{F}}_4]$.

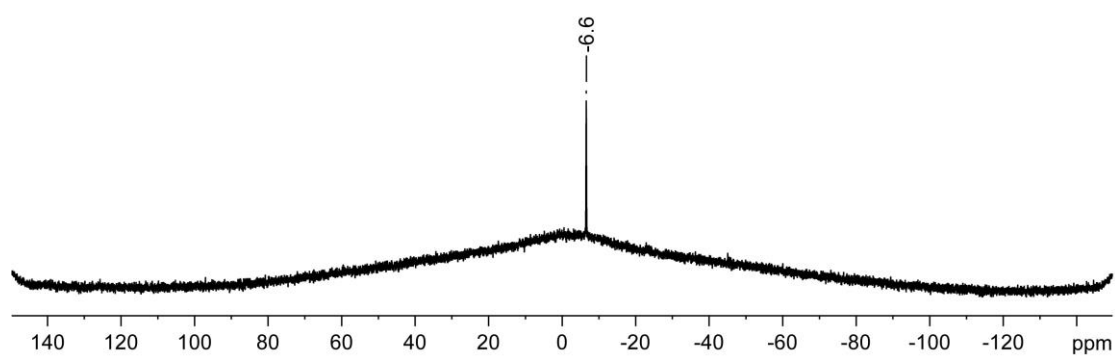


Figure S18. ^{11}B NMR spectrum (64.2 MHz, CD_2Cl_2) of $4[\text{BAr}^{\text{F}}_4]$.

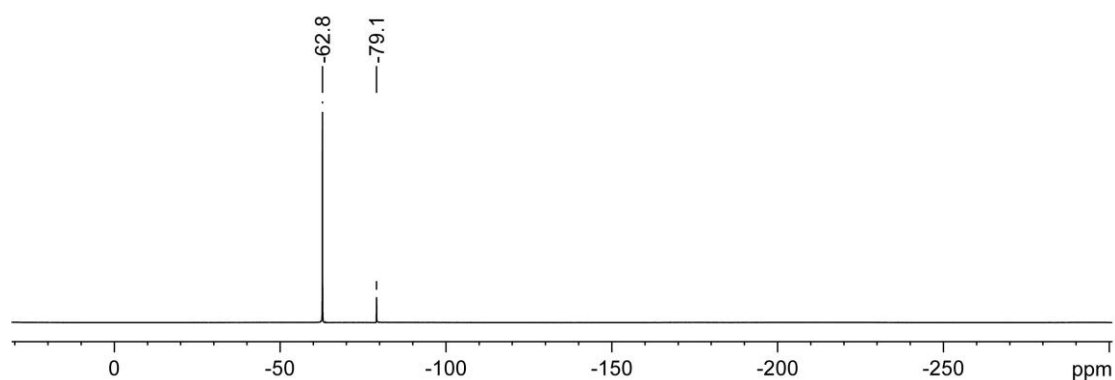


Figure S19. ^{19}F NMR spectrum (188.3 MHz, CD_2Cl_2) of $4[\text{BAr}^{\text{F}}_4]$.

C:\Users\Tatsumi\Desktop\TO710_Spritze
Solvent: MeCN

28.09.2015 14:28:43

TO710

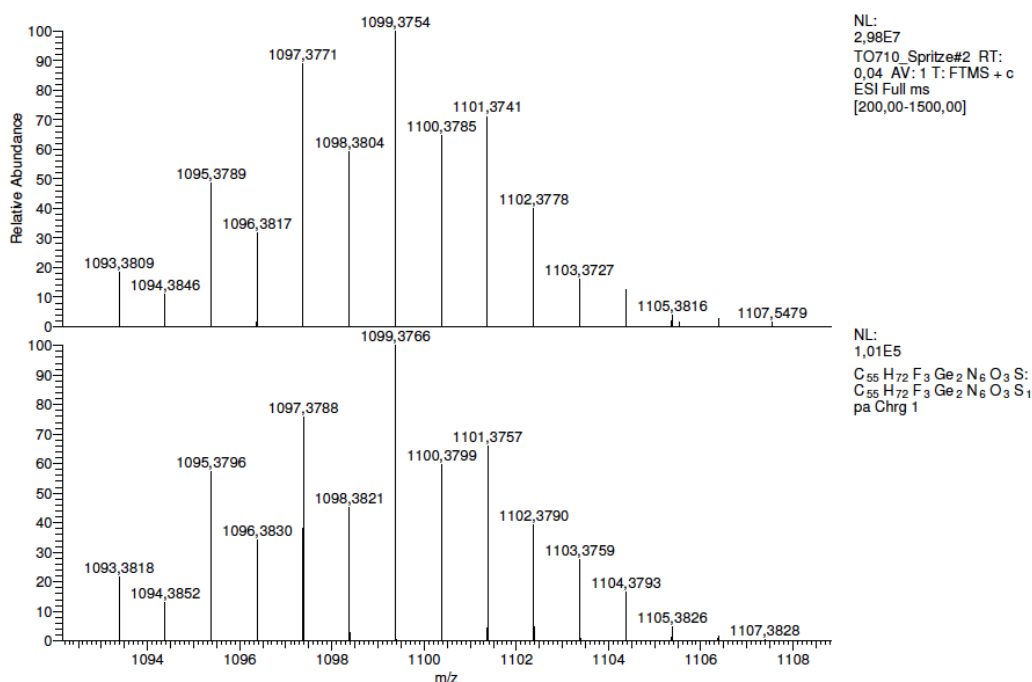


Figure S20. Signal of $[M - \text{BARF}_4]^+$ as observed in the ESI-HRMS (positive ion mode) analysis of $4[\text{BARF}_4]$. Top (expt.), bottom (calc.).

C:\Users\...TO715_Anionen_Spritze
Solvent: MeCN

30.09.2015 16:42:31

TO715_Anionen

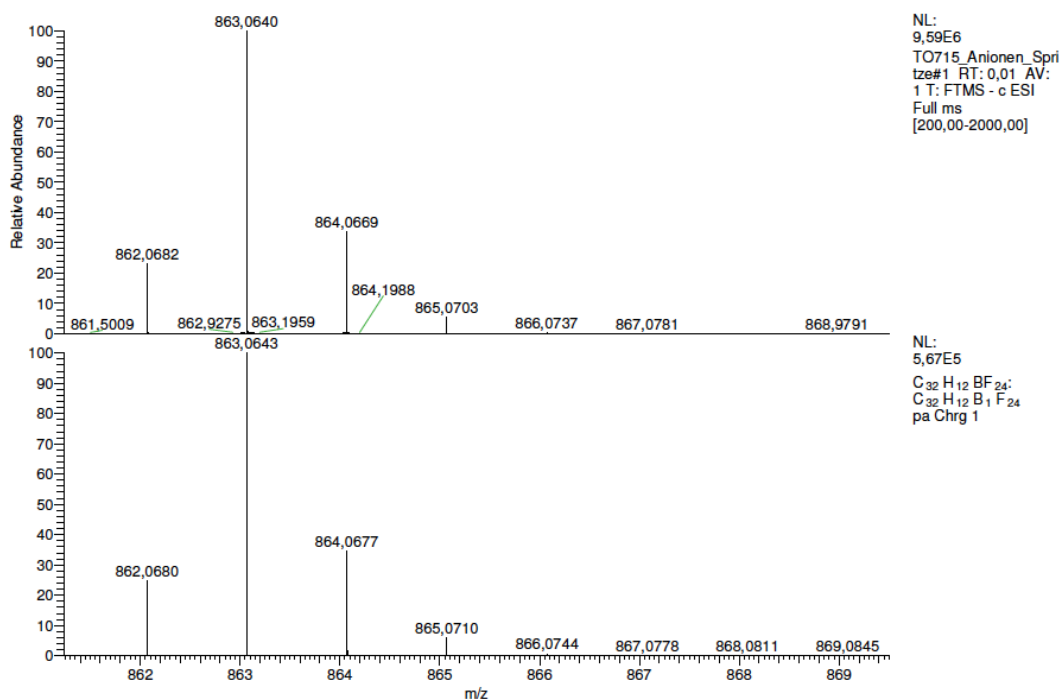


Figure S21. Signal of $[\text{BARF}_4]^-$ as observed in the ESI-HRMS (negative ion mode) analysis of $4[\text{BARF}_4]$. Top (expt.), bottom (calc.).

Synthetic Procedure and Analytical Data for 4[Al(OR^F)₄]

A Schlenk tube equipped with a PTFE-coated magnetic stirring bar was charged with 4[OTf] (222 mg, 0.178 mmol) and Ag[Al(OR^F)₄] (315 mg, 0.355 mmol). CH₂Cl₂ (10 ml) was transferred to the reaction vessel by cannula at -30 °C and the resulting mixture was stirred for 12 h while allowed to slowly warm to room temperature. The volatiles were removed under reduced pressure and recrystallization of the residue from CH₂Cl₂ at -30 °C afforded 4[Al(OR^F)₄] as colorless crystals (146 mg, 42%).

¹H NMR (200.1 MHz, CD₂Cl₂): δ = 1.28 (t, ³J_{HH} = 7 Hz, 48H, CH(CH₃)₂), 2.55 (sept, ³J_{HH} = 7 Hz, 8H, CH(CH₃)₂), 7.04 (s, 4H, NCH), 7.45 (d, ³J_{HH} = 8 Hz, 8H, Ar-H), 7.68 (t, ³J_{HH} = 8 Hz, 4H, Ar-H). ¹³C{¹H} NMR (100.6 MHz, CD₂Cl₂): δ = 23.7 (CH(CH₃)₂), 24.2 (CH(CH₃)₂), 29.7 (CH(CH₃)₂), 119.3 (NCH), 121.7 (q, ¹J_{CF} = 290 Hz, SO₃CF₃), 126.0 (Ar-C), 126.9 (Ar-C), 133.5 (Ar-C), 146.9 (Ar-C), 149.1 (NCN), n.o. (CCF₃), n.o. (CCF₃). ¹⁹F NMR (188.3 MHz, CD₂Cl₂): δ = -78.0 (SO₃CF₃), -75.7 (CCF₃). ESI-HRMS: *m/z* (positive ion mode): 1115.3232 (calc. 1115.3715 for [M + OH - H - Al{OC(CF₃)₃]₄]⁺). 967.4222 (calc. 967.4273 for [M + OH - OTf - Al{OC(CF₃)₃]₄]⁺). ESI-HRMS: *m/z* (negative ion mode): 966.9036 (calc. 966.9032 for [Al{OC(CF₃)₃]₄]⁻). M.p. at 206-208 °C (dec.).

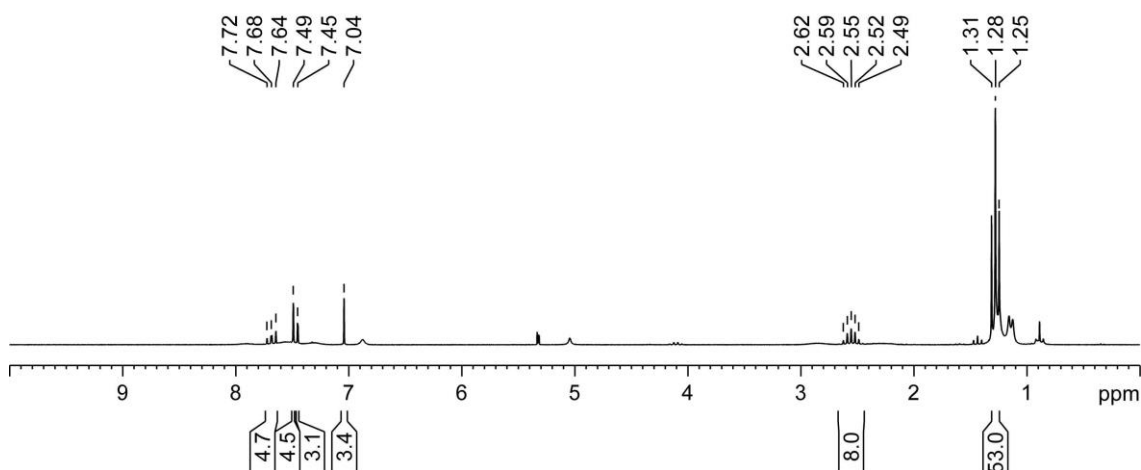


Figure S22. ¹H NMR spectrum (200.1 MHz, CD₂Cl₂) of 4[Al(OR^F)₄]. Mind the presence of hexane

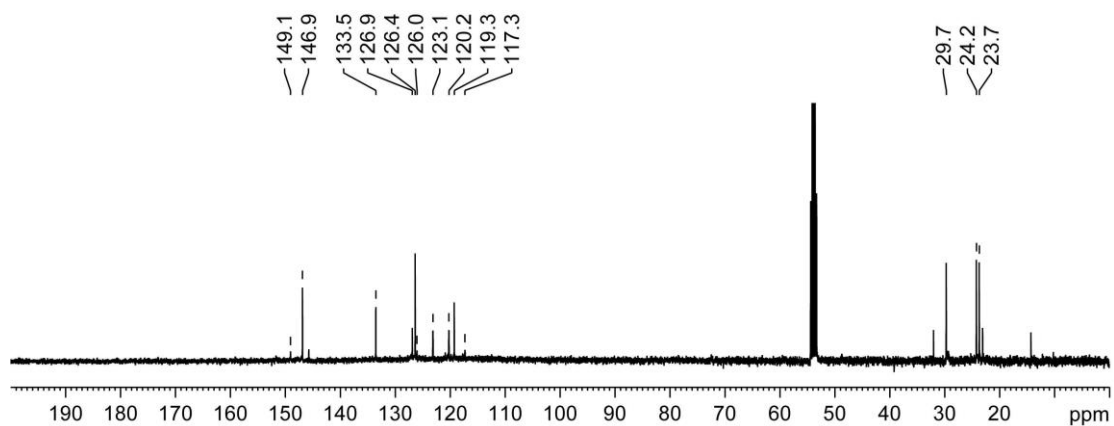


Figure S23. $^{13}\text{C}\{^1\text{H}\}$ NMR spectrum (100.6 MHz, CD_2Cl_2) of $4[\text{Al}(\text{OR}^{\text{F}})_4]$. Mind the presence of hexane

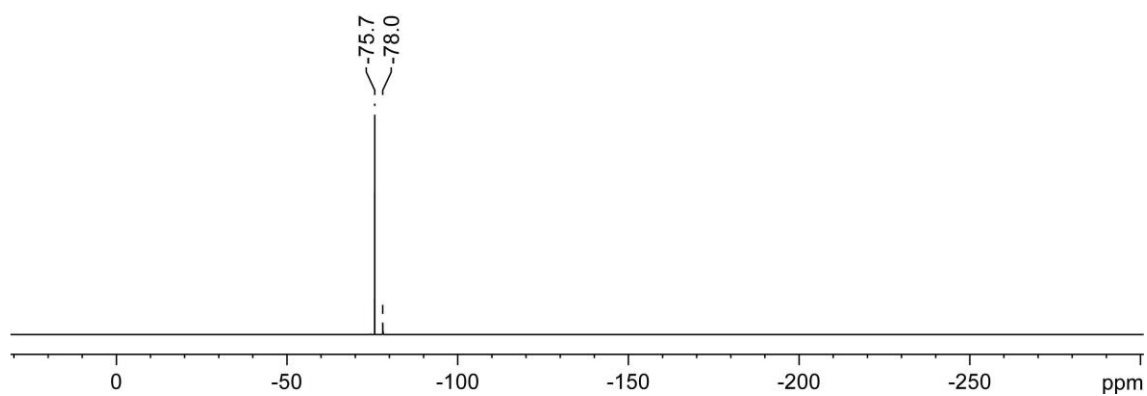


Figure S24. ^{19}F NMR spectrum (188.3 MHz, CD_2Cl_2) of $4[\text{Al}(\text{OR}^{\text{F}})_4]$.

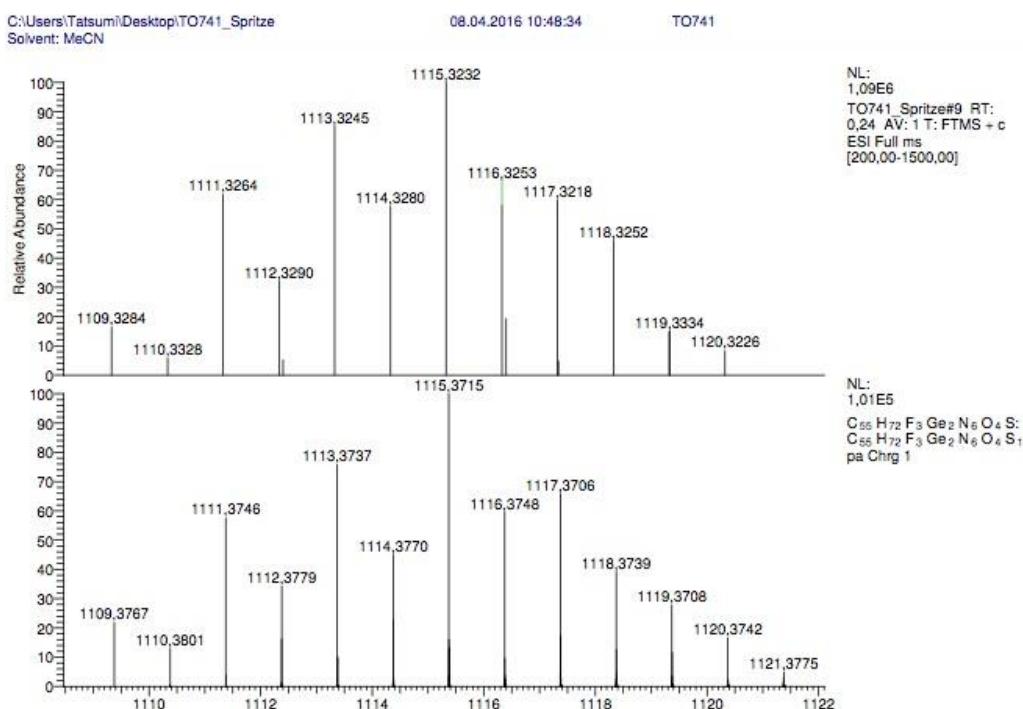


Figure S25. Signal of $[M + OH - H - Al(OR^F)_4]^+$ as observed in the ESI-HRMS (positive ion mode) analysis of $4[Al(OR^F)_4]$. Top (expt.), bottom (calc.).

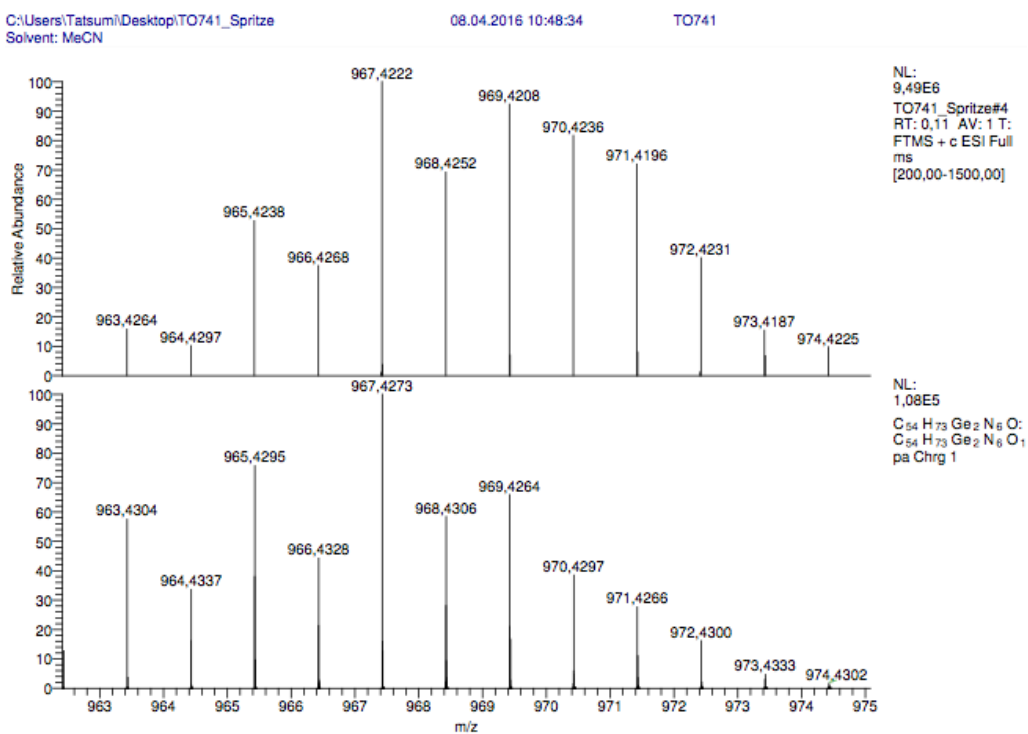


Figure S26. Signal of $[M + OH - OTf - Al(OR^F)_4]^+$ as observed in the ESI-HRMS (positive ion mode) analysis of $4[Al(OR^F)_4]$. Top (expt.), bottom (calc.).

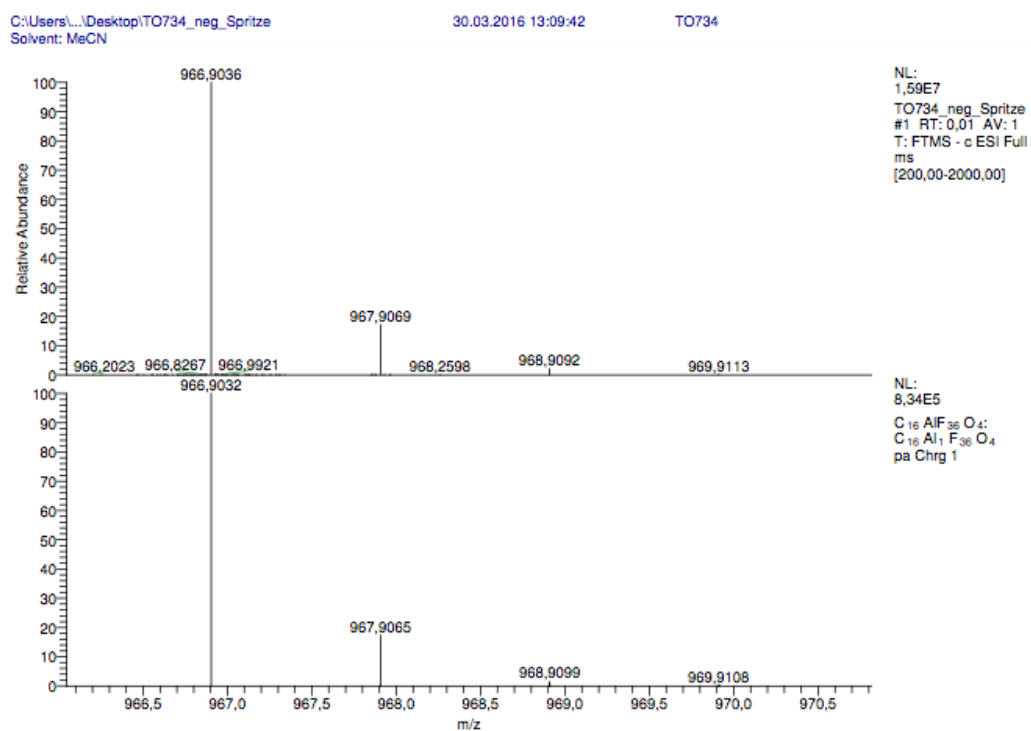


Figure S27. Signal of $[\text{Al}(\text{OR}^{\text{F}})_4]^-$ as observed in the ESI-HRMS (negative ion mode) analysis of $4[\text{Al}(\text{OR}^{\text{F}})_4]$. Top (expt.), bottom (calc.).

2.) Crystallographic Data for **3**[BF₄], **3**[BAr^F₄], **4**[BAr^F₄] and **4**[Al(OR^F)₄]

General Considerations: Data for the single crystal structure determinations of **3**[BF₄], **3**[BAr^F₄], **4**[BAr^F₄] and **4**[Al(OR^F)₄] were collected on an Agilent SuperNova diffractometer, equipped with a CCD area Atlas detector and a mirror monochromator utilizing CuK_α radiation ($\lambda = 1.54184 \text{ \AA}$). The crystal structures were solved by Direct Methods and refined on F² using full-matrix least squares with SHELXL-97^[S2]. The positions of the H atoms at the carbon atoms were calculated by standard methods. CCDC deposition numbers: 1448465 for **3**[BF₄], 1448464 for **3**[BAr^F₄], 1448466 for **4**[BAr^F₄] 1484307 for **4**[Al(OR^F)₄].

Table S1. Crystal data and structure refinement for **3**[BF₄].

Empirical formula	C ₁₂₈ H ₁₇₆ B ₂ F ₁₀ Ge ₄ N ₁₂ O ₅	
Formula weight	2464.79	
Temperature	150.00(10) K	
Wavelength	1.54184 Å	
Crystal system	Triclinic	
Space group	<i>P</i> -1	
Unit cell dimensions	a = 12.8884(4) Å	$\alpha = 80.538(2)^\circ$.
	b = 13.0569(4) Å	$\beta = 81.533(2)^\circ$.
	c = 20.9504(6) Å	$\gamma = 68.424(3)^\circ$.
Volume	3219.44(17) Å ³	
Z	1	
Density (calculated)	1.271 Mg/m ³	
Absorption coefficient	1.648 mm ⁻¹	
F(000)	1296	
Crystal size	0.35 x 0.30 x 0.23 mm ³	
Theta range for data collection	3.67 to 67.50°.	
Index ranges	-15 ≤ h ≤ 13, -15 ≤ k ≤ 14, -23 ≤ l ≤ 25	
Reflections collected	23900	
Independent reflections	11605 [R(int) = 0.0293]	
Completeness to theta = 67.50°	99.8 %	
Absorption correction	Semi-empirical from equivalents	
Max. and min. transmission	0.7071 and 0.5963	
Refinement method	Full-matrix least-squares on F ²	
Data / restraints / parameters	11605 / 219 / 800	
Goodness-of-fit on F ²	1.052	

Final R indices [$I > 2\sigma(I)$]	R1 = 0.0791, wR2 = 0.1874
R indices (all data)	R1 = 0.0905, wR2 = 0.1987
Largest diff. peak and hole	1.069 and -0.919 e.Å ⁻³

Table S2. Crystal data and structure refinement for **3**[BAR^F₄].

Empirical formula	C ₈₆ H ₈₄ BF ₂₅ Ge ₂ N ₆
Formula weight	1832.58
Temperature	150.00(10) K
Wavelength	1.54184 Å
Crystal system	Orthorhombic
Space group	<i>P</i> 212121
Unit cell dimensions	a = 19.34590(10) Å α = 90°. b = 20.75270(10) Å β = 90°. c = 21.57030(10) Å γ = 90°.
Volume	8660.04(7) Å ³
Z	4
Density (calculated)	1.406 Mg/m ³
Absorption coefficient	1.741 mm ⁻¹
F(000)	3744
Crystal size	0.41 x 0.30 x 0.14 mm ³
Theta range for data collection	2.95 to 67.50°.
Index ranges	-22 ≤ h ≤ 23, -14 ≤ k ≤ 24, -25 ≤ l ≤ 25
Reflections collected	33598
Independent reflections	15403 [R(int) = 0.0389]
Completeness to theta = 67.50°	100.0 %
Absorption correction	Semi-empirical from equivalents
Max. and min. transmission	0.7926 and 0.5383
Refinement method	Full-matrix least-squares on F ²
Data / restraints / parameters	15403 / 446 / 1291
Goodness-of-fit on F2	1.055
Final R indices [$I > 2\sigma(I)$]	R1 = 0.0519, wR2 = 0.1332
R indices (all data)	R1 = 0.0547, wR2 = 0.1364
Absolute structure parameter	-0.016(17)
Largest diff. peak and hole	0.842 and -0.710 e.Å ⁻³

Table S3. Crystal data and structure refinement for **4**[BAR^F₄].

Empirical formula	C ₈₉ H ₈₇ BF ₂₇ Ge ₂ N ₇ O ₃ S
Formula weight	2003.71
Temperature	150.00(10) K
Wavelength	1.54184 Å
Crystal system	Triclinic

Space group	<i>P</i> -1
Unit cell dimensions	$a = 12.9054(4) \text{ \AA}$ $\alpha = 89.046(2)^\circ$. $b = 16.9468(4) \text{ \AA}$ $\beta = 73.524(2)^\circ$. $c = 22.4045(4) \text{ \AA}$ $\gamma = 88.226(2)^\circ$.
Volume	$4696.4(2) \text{ \AA}^3$
Z	2
Density (calculated)	1.417 Mg/m^3
Absorption coefficient	1.917 mm^{-1}
F(000)	2044
Crystal size	$0.31 \times 0.20 \times 0.07 \text{ mm}^3$
Theta range for data collection	2.61 to 67.50° .
Index ranges	$-15 \leq h \leq 15$, $-20 \leq k \leq 20$, $-26 \leq l \leq 19$
Reflections collected	32602
Independent reflections	16923 [R(int) = 0.0308]
Completeness to theta = 67.50°	99.9 %
Absorption correction	Semi-empirical from equivalents
Max. and min. transmission	0.8839 and 0.5897
Refinement method	Full-matrix least-squares on F^2
Data / restraints / parameters	16923 / 102 / 1226
Goodness-of-fit on F^2	1.096
Final R indices [$I > 2\sigma(I)$]	R1 = 0.0487, wR2 = 0.1235
R indices (all data)	R1 = 0.0612, wR2 = 0.1343
Largest diff. peak and hole	1.287 and $-0.684 \text{ e.\AA}^{-3}$

Table S4. Crystal data and structure refinement for $4[\text{Al}(\text{OR}^F)_4]$

Empirical formula	$\text{C}_{284}\text{H}_{288}\text{Al}_4\text{F}_{156}\text{Ge}_8\text{N}_{24}\text{O}_{28}\text{S}_4$
Formula weight	8266.26
Temperature	$150.00(10) \text{ K}$
Wavelength	1.54184 \AA
Crystal system	Orthorhombic
Space group	<i>P</i> 212121
Unit cell dimensions	$a = 23.0848(3) \text{ \AA}$ $\alpha = 90^\circ$. $b = 26.6977(3) \text{ \AA}$ $\beta = 90^\circ$. $c = 27.5856(4) \text{ \AA}$ $\gamma = 90^\circ$.
Volume	$17001.3(4) \text{ \AA}^3$
Z	2
Density (calculated)	1.615 Mg/m^3
Absorption coefficient	2.475 mm^{-1}
F(000)	8320
Crystal size	$0.27 \times 0.18 \times 0.10 \text{ mm}^3$
Theta range for data collection	2.50 to 67.49° .
Index ranges	$-26 \leq h \leq 27$, $-31 \leq k \leq 31$, $-33 \leq l \leq 33$

Reflections collected	67376
Independent reflections	30534 [R(int) = 0.0740]
Completeness to theta = 67.49°	100.0 %
Absorption correction	Semi-empirical from equivalents
Max. and min. transmission	0.7864 and 0.5525
Refinement method	Full-matrix-block least-squares on F ²
Data / restraints / parameters	30534 / 314 / 2326
Goodness-of-fit on F2	1.083
Final R indices [I>2sigma(I)]	R1 = 0.0707, wR2 = 0.1770
R indices (all data)	R1 = 0.1169, wR2 = 0.1969
Absolute structure parameter	0.37(7)
Largest diff. peak and hole	1.350 and -0.794 e.Å ⁻³

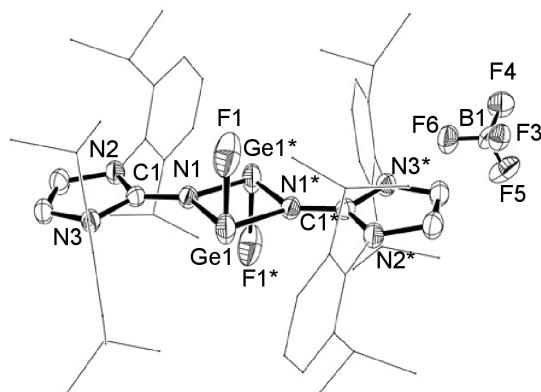
2.1.) Molecular Structure of $3[\text{BF}_4]$ in the Solid State

Figure S28. ORTEP representation of the molecular structure of $3[\text{BF}_4]$ in the solid state. Thermal ellipsoids are at the 40% probability level. Fluorine atoms have 50% occupancies for the F1 or F1* positions. Dip groups are depicted as stick models. Hydrogen atoms are omitted for clarity. Selected bond lengths (Å) and bond angles (deg): Ge1–F1, 1.894(8); Ge1–N1, 1.965(3); Ge1–N1*, 1.961(3); N1–C1, 1.320(5); N2–C1, 1.363(5); N3–C1, 1.360(5); F1–Ge1–N1, 92.0(2); F1–Ge1–N1*, 93.3(2); N1*–Ge1–N1, 79.39(14); Ge1*–N1–Ge1, 100.62(14)

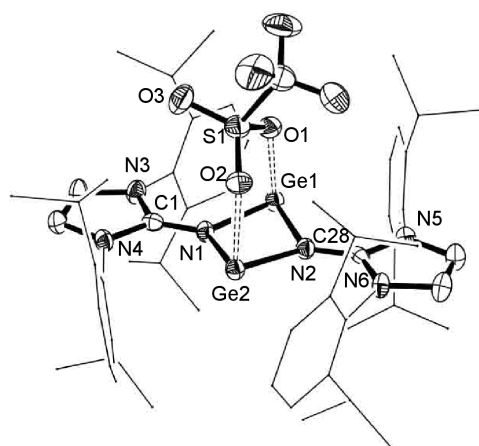


Figure S29. ORTEP representation of the molecular structure of $4[\text{Al}(\text{OR}^{\text{F}})_4]$ in the solid state. Thermal ellipsoids are at the 40% probability level. Dip groups are depicted as stick models. Hydrogen atoms are omitted for clarity. Selected bond lengths (Å) and bond angles (deg): Ge1–N1, 1.961(6); Ge1–N2, 1.961(6); Ge1–O1, 2.284(6); Ge2–N2, 1.958(6); Ge2–N1, 1.964(6); Ge2–O2, 2.244(5); N1–C1, 1.327(10); N3–C1, 1.377(10); N4–C1, 1.378(9); N2–C28, 1.333(10); N5–C28, 1.351(10); N6–C28, 1.380(10); N1–Ge1–N2, 78.5(3); N1–Ge1–O1, 88.3(2); N2–Ge1–O1, 88.0(2); N1–Ge2–N2, 78.5(2); N2–Ge2–O2, 88.7(2); N1–Ge2–O2, 90.4(2); C1–N1–Ge1, 128.3(5); C1–N1–Ge2, 130.4(5); Ge1–N1–Ge2, 100.6(3); C28–N2–Ge2, 129.6(5); C28–N2–Ge1, 128.2(5); Ge2–N2–Ge1, 100.8(3).

3.) Details to the DFT Calculations

DFT calculations for electronic structure analysis were performed at the B3LYP/6-31G* level of theory while energy differences were calculated at B97-D/6-31G* level.^[S3,S4,S5] Stationary points on the potential energy surface (PES) were characterized by harmonic vibrational frequency calculations. We calculated the electronic structure analysis part at B97-D/6-31G* level, as well and found generally negligible difference compared to B3LYP/6-31G* supporting that our results are independent from the chosen method. All calculations were carried out using GAUSSIAN 09 program.^[S6]

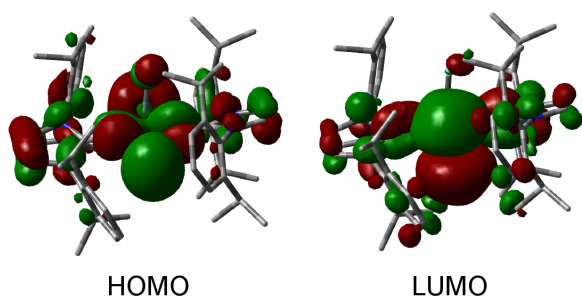


Figure S30. Kohn-Sham depictions of HOMO and LUMO of germyliumylidene 3^+ .

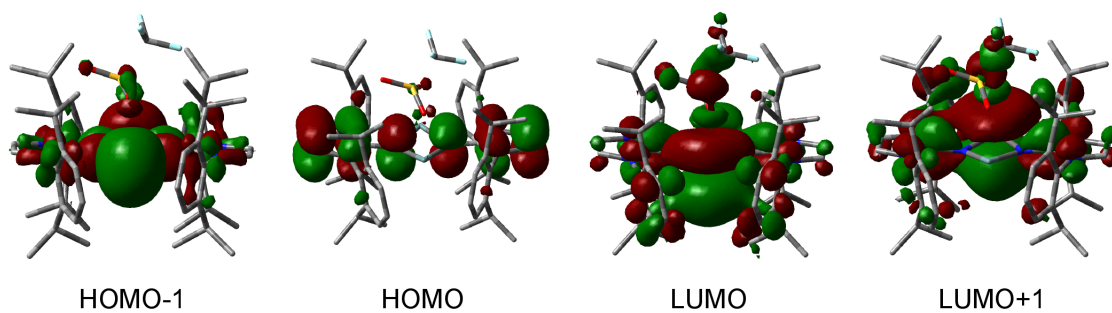


Figure S31. Kohn-Sham depictions of molecular orbitals (HOMO-1, HOMO, LUMO, LUMO+1) of Ge(II) cation 4^+ .

Table S5. Selected values for the MBOs in **3⁺**, **4⁺**, **V** and **VI**.

	Ge-N	Ge-F	Ge-O	C=N _{imino}
[FGe(NIPr) ₂ Ge] ⁺ (3⁺) Ge(F)-N _{imino} /Ge-N _{imino} :	0.55/0.89	0.79	–	1.32
[(OTf)Ge ₂ (NIPr) ₂] ⁺ (4⁺)	0.74	–	0.32	1.29
amino(imino)Ge(II) ⁺ (V) Ge-N _{imino} /Ge-N _{amino} :	0.68/1.11	–	–	1.24
Ge(NIPr) ₂ (VI)	1.12	–	–	1.55

Table S6. Selected values for the NPA Charges of **3⁺**, **4⁺**, **V** and **VI**.

	Ge(F)	Ge	F	N _{imino}	N _{amino}	O _{triflate}
[FGe(NIPr) ₂ Ge] ⁺ (3⁺)	+1.23	+1.10	-0.72	-1.16	–	–
[(OTf)Ge ₂ (NIPr) ₂] ⁺ (4⁺)	–	+1.20	–	-1.20	–	-0.95
amino(imino)Ge(II) ⁺ (V)	–	+1.15	–	-1.60	-1.69	–
Ge(NIPr) ₂ (VI)	–	+0.94	–	-0.99	–	–

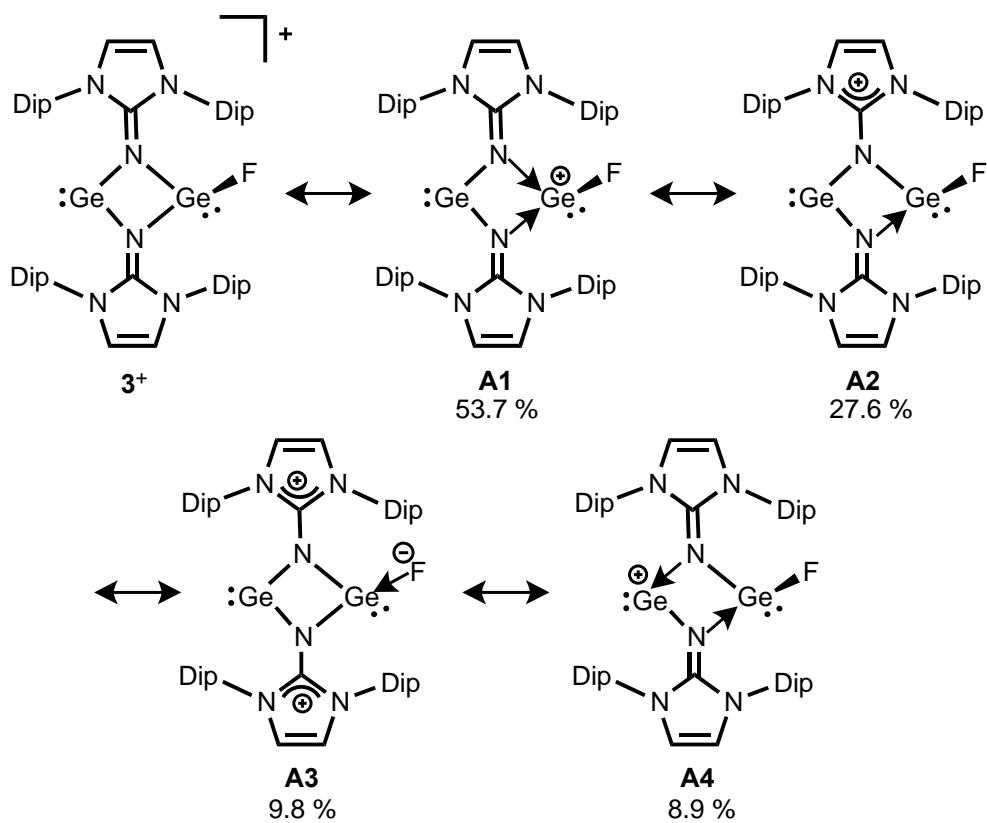


Figure S32. NRT-analysis of $[FGe(NIPr)_2Ge]^+$ (3^+).

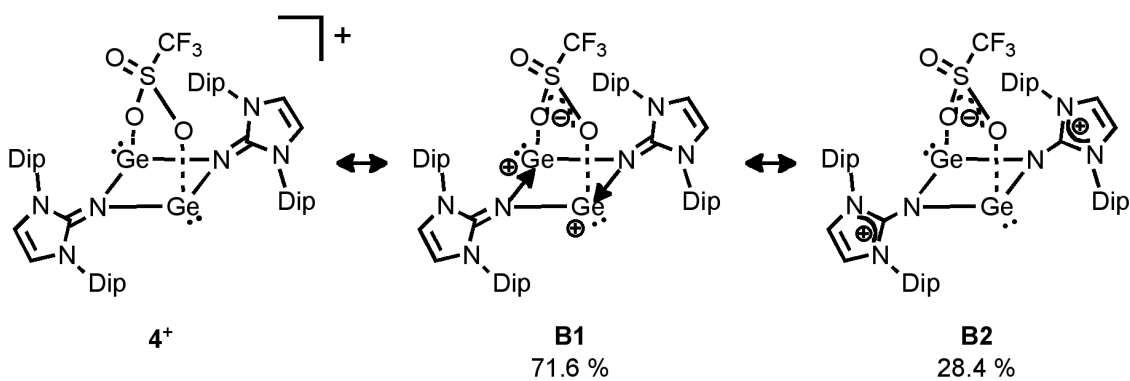


Figure S33. NRT-analysis of $[(OTf)Ge_2(NIPr)_2]^+$ (4^+).

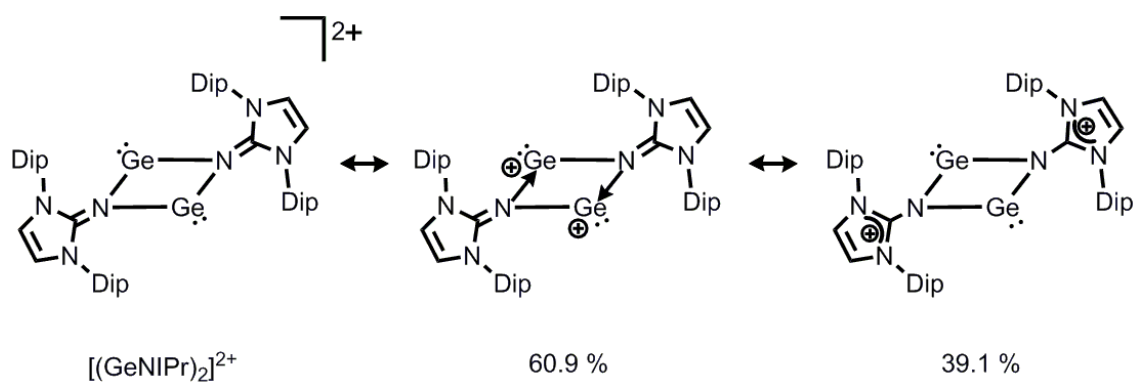


Figure S34. NRT-analysis of dicationic model compound $[(\text{GeNIPr})_2]^{2+}$.

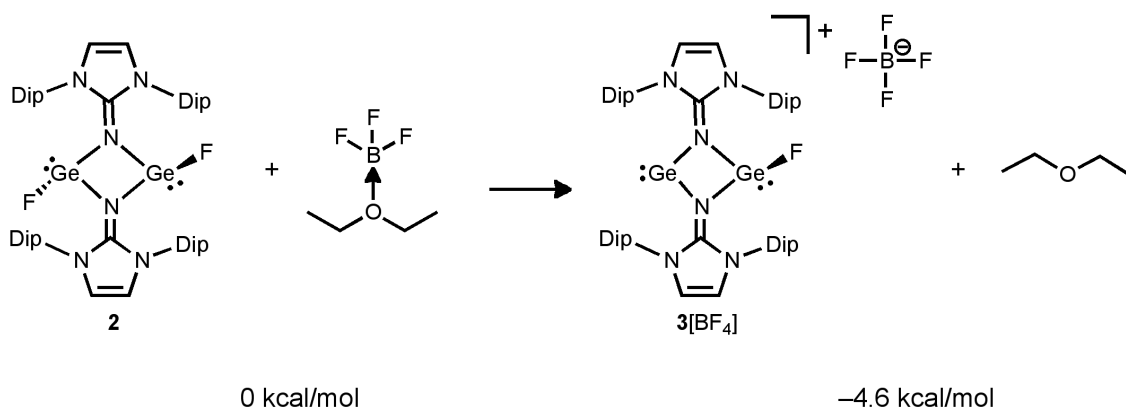


Figure S35. Calculated mechanism of the formation of **3**[BF₄] from germylene fluoride dimer **2**.

Calculation of the reaction free energy occurred at B97-D/6-31G* level of theory. In this case dispersion correction is mandatory to describe the system accurately. Ion-pairs were calculated together and the position of the BF₄⁻ anion was carefully optimized.

Table S7. Cartesian geometry of **2** at B97-D/6-31G* level in Angstrom [Å].

C	-1.817833	3.119603	1.852795
C	-2.67224	2.645463	0.826823
C	-2.96042	3.390675	-0.337915
C	-2.415882	4.685507	-0.432714
C	-1.593339	5.192031	0.578101
C	-1.291662	4.413497	1.704661
N	-3.204945	1.317397	0.935695
C	-2.503152	0.160727	0.601249
N	-3.41337	-0.876312	0.831219
C	-4.647779	-0.350088	1.235436
C	-4.519083	1.000292	1.300932
N	-1.276074	0.06059	0.171757
Ge	0.002656	1.495796	-0.501855
F	-0.208718	1.014921	-2.293918
C	-3.235884	-2.197536	0.290893
C	-2.774446	-3.231348	1.139571
C	-2.574963	-4.499002	0.56535

C	-2.790509	-4.712725	-0.802629
C	-3.239877	-3.668365	-1.619537
C	-3.48356	-2.388944	-1.086893
C	-2.49575	-2.963495	2.617806
C	-1.353686	-3.83068	3.186125
C	-4.004986	-1.274394	-1.989843
C	-5.371409	-1.660784	-2.602021
C	-3.805612	2.826678	-1.476967
C	-3.097925	2.963235	-2.844286
C	-1.452171	2.222931	3.035906
C	-2.603147	2.175597	4.069725
N	1.264405	-0.069433	-0.184122
Ge	-0.015705	-1.518169	0.464159
F	0.209303	-1.068548	2.260871
C	2.496216	-0.153207	-0.602369
N	3.402971	0.894403	-0.798707
C	4.643823	0.382858	-1.203388
C	4.52278	-0.966252	-1.301268
N	3.207117	-1.298073	-0.955497
C	3.226071	2.199693	-0.218472
C	2.770694	3.260494	-1.036637
C	2.594169	4.516512	-0.42989
C	2.825671	4.693827	0.9407
C	3.260934	3.621731	1.728536
C	3.48094	2.352036	1.162868
C	2.471878	3.033954	-2.517751
C	3.755408	3.220013	-3.361641
C	3.98462	1.20745	2.037442
C	5.366855	1.547192	2.641548
C	2.679342	-2.630744	-0.883888
C	2.966904	-3.405878	0.261283
C	2.430508	-4.706204	0.31848

C	1.617745	-5.191008	-0.710593
C	1.317411	-4.384155	-1.817404
C	1.834584	-3.082832	-1.927602
C	3.804473	-2.86936	1.419023
C	3.085066	-3.034307	2.776982
C	1.47142	-2.159501	-3.090745
C	2.629936	-2.077338	-4.113976
C	5.195419	-3.544454	1.441359
C	0.163319	-2.562043	-3.799288
C	2.967584	0.848122	3.142319
C	1.335045	3.932147	-3.047741
C	-3.787795	-3.149048	3.449157
C	-2.985302	-0.911806	-3.090764
C	-5.1983	3.498054	-1.502857
C	-0.134755	2.630997	3.723603
H	-5.4909	-1.001743	1.428088
H	-3.409782	-3.838675	-2.684406
H	-2.604257	-5.699344	-1.233483
H	-4.167508	-0.374562	-1.381392
H	-3.385133	-0.094906	-3.71404
H	-2.033678	-0.578599	-2.655546
H	-2.79387	-1.778445	-3.744204
H	-5.2747	-2.549168	-3.247602
H	-6.111285	-1.886995	-1.816814
H	-5.755032	-0.830833	-3.218349
H	1.054681	3.603243	-4.06016
H	-4.158794	-4.184055	3.358662
H	-3.587215	-2.944295	4.513975
H	-4.58263	-2.46598	3.110582
H	-3.726003	2.507396	-3.627746
H	-0.126363	-1.765641	-4.501044
H	-0.653509	-2.697389	-3.075639

H	5.22689	-1.733303	-1.599408
H	-2.209031	-5.315914	1.187356
H	2.137375	1.992763	-2.635462
H	-0.454305	-3.749188	2.558698
H	-1.648714	-4.891568	3.258897
H	2.637338	-5.328506	1.190872
H	1.196824	-6.196926	-0.643449
H	0.650507	-4.764226	-2.590637
H	3.958983	-1.792853	1.263353
H	5.095007	-4.632501	1.589869
H	5.803599	-3.137916	2.266588
H	5.734988	-3.37771	0.494678
H	2.925419	-4.098957	3.015231
H	2.112429	-2.521316	2.77373
H	1.305239	-1.1528	-2.679789
H	0.286081	-3.496912	-4.373328
H	3.559075	-1.718717	-3.645971
H	2.363213	-1.381401	-4.92655
H	2.821339	-3.069995	-4.556044
H	-5.216842	1.777686	1.58683
H	2.235013	5.353796	-1.028369
H	-2.178337	-1.914723	2.712557
H	0.448065	3.859296	-2.400855
H	1.649309	4.988283	-3.108255
H	-2.62305	5.286106	-1.320052
H	-1.164993	6.192283	0.480591
H	-0.614655	4.808352	2.461525
H	-3.955818	1.75332	-1.296087
H	-5.101069	4.582915	-1.675017
H	-5.811786	3.072946	-2.314692
H	-5.730384	3.350139	-0.548857
H	-2.946583	4.022674	-3.109562

H	-2.122149	2.456207	-2.83697
H	-1.298688	1.205011	2.647827
H	-0.242284	3.585238	4.267912
H	-3.538664	1.813466	3.617425
H	-2.336077	1.497786	4.8974
H	-2.782918	3.180423	4.488514
H	5.48538	1.042915	-1.373038
H	3.438054	3.762825	2.796454
H	2.660111	5.672756	1.396861
H	4.118113	0.31644	1.410066
H	3.354758	0.010658	3.745884
H	2.004262	0.544488	2.71094
H	2.802869	1.706851	3.813304
H	5.299743	2.423513	3.307104
H	6.103039	1.771751	1.852421
H	5.736934	0.694937	3.235339
H	-1.101805	-3.479409	4.198622
H	3.709074	-2.601081	3.576436
H	0.148372	1.854402	4.4499
H	0.679744	2.732202	2.991834
H	3.536845	3.046727	-4.428471
H	4.145231	4.245907	-3.249325
H	4.542413	2.514537	-3.052021

Table S8. Cartesian geometry of $\mathbf{3}^+$ at B97-D/6-31G* level in Angstrom [\AA].

C	-2.384404	-4.793429	-1.22454
C	-2.46152	-3.805282	-2.215813
C	-2.821066	-2.484703	-1.896788
C	-3.102443	-2.209479	-0.536543
C	-2.999103	-3.173202	0.492564
C	-2.647216	-4.481393	0.114565
C	-2.894672	-1.385283	-2.957179

C	-4.363408	-1.138776	-3.384254
N	-3.47931	-0.867586	-0.168203
C	-2.589095	0.157214	0.073098
N	-3.369777	1.239231	0.43955
C	-4.717818	0.873438	0.452484
C	-4.783106	-0.434688	0.082928
N	-1.270462	0.095307	-0.011798
Ge	-0.037815	-1.596984	0.075232
F	0.170925	-1.733895	-1.731053
C	-2.806965	2.477936	0.897639
C	-2.739115	3.566796	-0.005704
C	-2.044505	4.710632	0.426281
C	-1.446626	4.759027	1.693959
C	-1.551868	3.672998	2.570956
C	-2.240336	2.504152	2.193285
C	-3.351556	3.475307	-1.405822
C	-2.377852	2.780394	-2.390631
C	-2.35451	1.332583	3.166906
C	-3.146875	1.755651	4.426677
C	-3.250482	-2.825372	1.957475
C	-4.642527	-3.333206	2.400401
N	1.255183	0.047866	0.075144
C	2.562265	0.006107	-0.123761
N	3.37883	1.008442	-0.609959
C	4.697834	0.556822	-0.691998
C	4.710009	-0.728292	-0.244213
N	3.400361	-1.068966	0.100661
C	2.884826	2.307897	-0.96657
C	2.94411	3.336604	0.00487
C	2.330656	4.559969	-0.319604
C	1.694839	4.743136	-1.554749
C	1.670319	3.711611	-2.50113

C	2.261683	2.462867	-2.228018
C	2.970045	-2.330992	0.647134
C	2.67322	-2.387919	2.031818
C	2.224596	-3.617858	2.542518
C	2.076196	-4.734255	1.707671
C	2.37136	-4.642981	0.343965
C	2.818888	-3.434929	-0.225257
C	3.5817	3.11835	1.377882
C	2.492267	2.862833	2.446763
C	2.838544	-1.160488	2.928126
C	1.965278	-1.207947	4.197545
C	3.129588	-3.345414	-1.71832
C	2.144011	-4.157432	-2.589483
C	2.210544	1.346649	-3.267411
C	3.032705	1.742233	-4.516823
Ge	0.028456	1.531751	0.013393
C	4.579685	-3.817238	-1.991491
C	0.755141	0.995573	-3.655766
C	4.327528	-0.962211	3.300885
C	-2.145988	-3.37967	2.886801
C	-0.967925	0.773976	3.558323
C	4.487189	4.296888	1.798847
C	-3.785114	4.845727	-1.96603
C	-2.027725	-1.670395	-4.199101
H	2.960688	2.712819	3.433166
H	1.801451	3.719816	2.50872
H	1.903126	1.96509	2.204913
H	5.000933	4.049521	2.740999
H	5.247685	4.511323	1.031986
H	3.902036	5.214244	1.969718
H	3.022811	0.918943	-5.248608
H	2.604867	2.635461	-4.999472

H	4.078799	1.964006	-4.251956
H	0.758123	0.200047	-4.416432
H	0.187749	0.619098	-2.792311
H	0.236404	1.872375	-4.074866
H	4.806705	-3.736852	-3.066681
H	5.32289	-3.223404	-1.437013
H	4.6977	-4.871495	-1.692109
H	2.337281	-3.936591	-3.65095
H	2.286153	-5.241151	-2.447578
H	1.104222	-3.892972	-2.357242
H	4.444814	-0.057198	3.91987
H	4.697052	-1.826212	3.876125
H	4.952118	-0.850191	2.401276
H	2.015563	-0.234628	4.709406
H	0.914837	-1.420072	3.946979
H	2.320447	-1.974806	4.904251
H	-2.305664	-3.005418	3.910955
H	-2.173721	-4.480102	2.926455
H	-1.147046	-3.072911	2.540733
H	-4.827216	-3.071361	3.454782
H	-5.444136	-2.892853	1.786244
H	-4.698818	-4.428938	2.299558
H	-4.406102	-0.32869	-4.130597
H	-4.783448	-2.049637	-3.840451
H	-4.997775	-0.854751	-2.531559
H	-2.030226	-0.782245	-4.850276
H	-0.99286	-1.900493	-3.912618
H	-2.436081	-2.510247	-4.784745
H	-2.833344	2.725934	-3.392914
H	-1.434003	3.344301	-2.464381
H	-2.138752	1.755289	-2.072188
H	-4.344115	4.697488	-2.902617

H	-4.428003	5.38855	-1.255899
H	-2.913677	5.478343	-2.199067
H	-3.252395	0.899	5.111416
H	-2.621739	2.561603	4.963094
H	-4.151463	2.119254	4.160107
H	-1.089266	-0.062359	4.264295
H	-0.42482	0.400257	2.676198
H	-0.351735	1.54565	4.046857
H	2.517636	-0.275738	2.361047
H	1.975144	-3.702744	3.599825
H	1.718016	-5.678013	2.123693
H	2.239243	-5.514947	-0.296177
H	3.041961	-2.290776	-2.023009
H	4.210775	2.217643	1.335082
H	2.345943	5.374029	0.406245
H	1.221764	5.700217	-1.782967
H	1.187352	3.870178	-3.46664
H	2.66598	0.441769	-2.839695
H	-3.246109	-1.728504	2.060805
H	-2.563693	-5.253518	0.880252
H	-2.103286	-5.812423	-1.497886
H	-2.222429	-4.060334	-3.247358
H	-2.509484	-0.461347	-2.498958
H	-2.91088	0.517437	2.681837
H	-4.251638	2.844722	-1.341712
H	-1.967819	5.572933	-0.235866
H	-0.906977	5.656176	2.003264
H	-1.102511	3.725859	3.563884
H	-5.486321	1.584423	0.730572
H	-5.622388	-1.10746	-0.039705
H	5.514978	-1.44231	-0.134677
H	5.486826	1.199157	-1.063936

Table S9. Cartesian geometry of 4^+ at B97-D/6-31G* level in Angstrom [Å].

C	3.617331	-1.423102	-0.359411
C	3.459787	-1.936474	-1.674389
C	3.462189	-3.333425	-1.822222
C	3.623574	-4.177742	-0.714804
C	3.792978	-3.641142	0.56451
C	3.792869	-2.248276	0.77644
C	3.29682	-1.008444	-2.879589
C	2.615027	-1.685133	-4.085322
C	4.026192	-1.678803	2.171853
C	3.303968	-2.478461	3.278839
N	3.585955	0.008622	-0.179792
C	2.45397	0.795354	-0.240398
N	2.902036	2.098097	-0.128457
C	4.295421	2.111441	-0.012759
C	4.716851	0.820394	-0.035452
C	2.076781	3.240409	-0.42979
C	1.539291	4.007936	0.632629
C	0.651121	5.0429	0.285674
C	0.309304	5.288118	-1.050484
C	0.877381	4.525817	-2.078367
C	1.788182	3.492855	-1.792492
N	1.194679	0.394676	-0.399201
Ge	0.464573	-1.462282	-0.279334
N	-1.21018	-0.365928	-0.442312
C	-2.476649	-0.765456	-0.400109
N	-3.611184	0.022133	-0.332568
C	-4.752894	-0.781373	-0.424783
C	-4.337969	-2.072724	-0.503394
N	-2.940186	-2.065522	-0.462406
C	-3.59976	1.462073	-0.38587
C	-3.608826	2.194093	0.829043

C	-3.492235	3.592372	0.731108
C	-3.382485	4.226315	-0.514277
C	-3.40807	3.477081	-1.694527
C	-3.521548	2.075011	-1.65731
C	1.928111	3.742677	2.083302
C	0.806013	4.06816	3.091697
C	2.425799	2.700662	-2.932587
C	3.225173	3.635811	-3.870046
C	-3.769576	1.494079	2.177004
C	-3.211371	2.30404	3.364098
C	-3.539775	1.282605	-2.961308
C	-4.734896	1.702907	-3.847426
C	-2.092035	-3.20135	-0.711879
C	-1.711586	-3.455379	-2.049328
C	-0.809603	-4.511835	-2.274019
C	-0.323011	-5.279107	-1.209703
C	-0.730714	-5.010676	0.104282
C	-1.621753	-3.960303	0.388829
C	-2.240245	-2.639734	-3.226402
C	-1.089414	-1.977631	-4.013386
C	-2.067329	-3.645936	1.815997
C	-3.444184	-4.294888	2.104702
Ge	-0.481126	1.476285	-0.233031
C	-5.263177	1.171254	2.437922
C	-2.204054	1.445793	-3.7169
C	-3.103679	-3.524753	-4.155509
C	5.546002	-1.629837	2.471061
C	1.369519	1.901473	-3.724941
C	3.203217	4.548194	2.439292
C	-1.051001	-4.08861	2.888924
C	4.660568	-0.41879	-3.315552
O	-0.426514	1.094492	2.04954

S	0.38171	0.047371	2.721294
C	-0.65204	-0.397387	4.246392
F	-0.783808	0.682399	5.036251
O	0.39276	-1.234284	1.960814
O	1.660417	0.476481	3.233761
F	-1.88308	-0.823556	3.877664
F	-0.042419	-1.379207	4.933475
H	-1.365782	-3.698295	3.867548
H	-1.00929	-5.187289	2.966986
H	-0.042246	-3.70978	2.672499
H	-3.765332	-4.050905	3.12997
H	-4.218383	-3.940107	1.408683
H	-3.373846	-5.391096	2.015395
H	-2.182671	-2.554261	1.895707
H	-0.336996	-5.613151	0.921974
H	0.381268	-6.090569	-1.40247
H	-0.493158	-4.731741	-3.294846
H	-1.494227	-1.375143	-4.841288
H	-0.495494	-1.318061	-3.362366
H	-0.418131	-2.737263	-4.442367
H	-3.506106	-2.921583	-4.985188
H	-2.501579	-4.341549	-4.584498
H	-3.946319	-3.972754	-3.605805
H	-2.884168	-1.835357	-2.843844
H	-4.886156	-3.002357	-0.58673
H	-5.741546	-0.34105	-0.427291
H	-2.229	0.888116	-4.666254
H	-2.007276	2.50556	-3.942859
H	-1.368543	1.063281	-3.113666
H	-4.759016	1.088708	-4.761745
H	-5.689293	1.57476	-3.312997
H	-4.650355	2.759254	-4.147803

H	-3.662527	0.215	-2.728779
H	-3.338628	3.978292	-2.661217
H	-3.285227	5.312559	-0.561348
H	-3.481187	4.192485	1.640019
H	-3.218009	0.543577	2.127346
H	-3.246581	1.686026	4.272477
H	-2.170866	2.610113	3.191481
H	-3.820827	3.20318	3.551384
H	-5.368594	0.65776	3.406913
H	-5.851995	2.102103	2.473803
H	-5.688444	0.522556	1.658939
H	1.851972	1.350554	-4.547801
H	0.863582	1.174077	-3.072721
H	0.609073	2.569834	-4.157386
H	3.713448	3.044169	-4.660886
H	2.562564	4.371445	-4.352578
H	4.0005	4.185464	-3.313908
H	3.139827	1.979842	-2.511624
H	0.625209	4.737409	-3.11889
H	-0.397063	6.084659	-1.292124
H	0.211582	5.651932	1.075206
H	3.49879	4.340225	3.47982
H	4.047074	4.286731	1.782529
H	3.013606	5.629481	2.339999
H	1.097524	3.69711	4.085668
H	0.642395	5.15532	3.174406
H	-0.141097	3.588555	2.807579
H	2.163738	2.674862	2.182515
H	4.837204	3.044632	0.070487
H	5.703933	0.383812	0.038655
H	2.36895	-0.924102	-4.841207
H	3.282671	-2.422665	-4.558993

H	1.687905	-2.195283	-3.788181
H	4.516892	0.26375	-4.169207
H	5.14217	0.144866	-2.503787
H	5.340678	-1.226488	-3.63033
H	2.652429	-0.172765	-2.574186
H	5.716937	-1.194057	3.46827
H	5.971366	-2.646651	2.459091
H	6.093081	-1.025056	1.731028
H	3.373515	-1.925046	4.226955
H	2.242134	-2.623309	3.038148
H	3.771869	-3.464916	3.430163
H	3.637317	-0.652634	2.199115
H	3.334116	-3.769385	-2.812198
H	3.62054	-5.260652	-0.854324
H	3.923729	-4.305921	1.418434

Table S10. Cartesian geometry of **V** at B97-D/6-31G* level in Angstrom [Å].

C	-3.715511	0.294399	0.993749
C	-2.967739	-0.223952	-0.09323
C	-3.271117	0.052442	-1.450716
C	-4.352663	0.916537	-1.698917
C	-5.0938	1.47145	-0.646247
C	-4.781111	1.159962	0.681552
N	-1.901182	-1.154723	0.196024
C	-0.548921	-0.936125	0.075791
N	0.054434	-2.115195	0.452671
C	-0.912942	-3.05311	0.815516
C	-2.123518	-2.45976	0.653181
N	0.096042	0.163096	-0.313343
Ge	2.082033	0.446435	-0.706108
N	1.521575	2.209149	-0.435242
Si	2.511772	3.674157	-0.374362

C	1.476454	-2.28851	0.572233
C	2.156019	-2.979749	-0.459401
C	3.557242	-3.051031	-0.360652
C	4.238203	-2.455477	0.711004
C	3.532684	-1.791932	1.722762
C	2.127578	-1.695613	1.681937
C	1.399882	-3.563047	-1.654789
C	2.094841	-4.791615	-2.278131
C	1.370606	-1.000836	2.811641
C	1.911194	0.420152	3.090042
C	-2.474861	-0.585872	-2.593272
C	-2.637934	0.136987	-3.946699
C	-3.474434	-0.122242	2.447028
C	-3.522117	1.048177	3.456623
C	1.172862	-2.472801	-2.731864
C	1.424573	-1.867899	4.09306
C	-2.854815	-2.078678	-2.765671
C	-4.535401	-1.17614	2.860527
H	0.610188	-2.893156	-3.580781
H	0.601904	-1.621247	-2.330905
H	2.139415	-2.099064	-3.106479
H	1.434312	-5.237028	-3.037278
H	3.033988	-4.510249	-2.780376
H	2.321798	-5.555912	-1.518814
H	0.40717	-3.888138	-1.305927
H	4.123606	-3.573883	-1.130673
H	5.326625	-2.518067	0.761216
H	4.071435	-1.351875	2.56288
H	0.855484	-1.381916	4.90141
H	0.997601	-2.867316	3.914273
H	2.465115	-1.994602	4.431451
H	1.312245	0.896675	3.882284

H	2.956361	0.387346	3.436097
H	1.864278	1.056507	2.192541
H	0.312909	-0.902459	2.525712
H	-0.630882	-4.044633	1.147224
H	-3.129874	-2.827351	0.797006
H	-1.932961	-0.294611	-4.673369
H	-3.654122	0.001607	-4.350232
H	-2.438803	1.21539	-3.863221
H	-2.259545	-2.520579	-3.580855
H	-2.673083	-2.663385	-1.852775
H	-3.920421	-2.16972	-3.029929
H	-1.407978	-0.534986	-2.326636
H	-4.331293	-1.538597	3.880497
H	-5.538169	-0.72039	2.849835
H	-4.557009	-2.041101	2.180606
H	-3.319863	0.658421	4.466584
H	-2.778766	1.823689	3.229575
H	-4.518169	1.516629	3.479317
H	-2.478772	-0.586471	2.523306
H	-4.617775	1.162816	-2.726054
H	-5.926502	2.142227	-0.865159
H	-5.377647	1.582115	1.490474
C	1.640971	5.042992	-1.331608
C	2.718013	4.164699	1.434772
C	4.18122	3.245725	-1.136675
H	2.256243	5.958692	-1.354494
H	1.442687	4.748316	-2.375572
H	0.676172	5.313547	-0.868693
H	4.873	4.103519	-1.084549
H	4.668685	2.407423	-0.607478
H	4.087245	2.962657	-2.199134
H	3.318951	5.084997	1.533602

H	1.744867	4.352008	1.919776
H	3.227516	3.370797	2.007204
Si	-0.194309	1.924231	-0.258146
C	-0.928732	2.501832	1.359613
C	-1.127113	2.627224	-1.716272
H	-2.215145	2.501676	-1.6246
H	-0.911824	3.706738	-1.788639
H	-0.797068	2.161127	-2.657872
H	-2.025269	2.421023	1.326433
H	-0.555229	1.928743	2.222278
H	-0.676947	3.563298	1.527399

Table S11. Cartesian geometry of **VI** at B97-D/6-31G* level in Angstrom [Å].

C	-0.265544	-3.519296	-0.455496
C	-1.263682	-2.97837	-1.298962
C	-1.16758	-3.014025	-2.710743
C	-0.055421	-3.662391	-3.276924
C	0.935418	-4.227858	-2.463613
C	0.835497	-4.1456	-1.068266
N	-2.401788	-2.355192	-0.699279
C	-2.362712	-1.063006	-0.130077
N	-3.634139	-0.93294	0.455798
C	-4.383217	-2.103434	0.28349
C	-3.621416	-2.982132	-0.421329
N	-1.391324	-0.222012	-0.071341
Ge	-0.021455	0.150295	-1.270377
N	1.357541	0.281389	-0.032594
C	2.343058	1.092685	0.10966
N	3.575349	0.811186	0.72465
C	4.356385	1.968708	0.817888
C	3.658145	2.988131	0.248517
N	2.442885	2.46609	-0.205973

C	3.891175	-0.458597	1.304404
C	3.741342	-0.623243	2.701261
C	4.096893	-1.868459	3.250911
C	4.569519	-2.905526	2.436765
C	4.674343	-2.72622	1.050532
C	4.331089	-1.499766	0.454114
C	3.128987	0.485375	3.557736
C	1.58475	0.365334	3.538346
C	4.446629	-1.270301	-1.052359
C	5.756087	-0.517601	-1.386714
C	1.376495	3.183077	-0.829618
C	0.232611	3.491156	-0.055483
C	-0.842886	4.119062	-0.708568
C	-0.776678	4.423314	-2.073428
C	0.375942	4.123958	-2.813689
C	1.477608	3.493058	-2.20869
C	0.189619	3.217032	1.445706
C	0.638891	4.487142	2.208592
C	2.728723	3.112149	-3.004872
C	2.973731	4.015669	-4.231392
C	-4.053299	0.221796	1.18902
C	-4.584452	1.322099	0.481578
C	-4.963476	2.458025	1.220738
C	-4.825671	2.48818	2.613259
C	-4.299071	1.380946	3.29325
C	-3.896862	0.227684	2.596276
C	-4.721254	1.316514	-1.038266
C	-3.71092	2.301523	-1.668717
C	-3.239978	-0.948974	3.320029
C	-3.830858	-1.209026	4.721876
C	-2.2378	-2.384748	-3.598145
C	-3.123846	-3.482445	-4.232444

C	-0.365032	-3.45534	1.065939
C	0.911764	-2.856998	1.692874
C	-1.18453	2.726958	1.941847
C	2.671489	1.62613	-3.433477
C	4.343992	-2.566878	-1.878614
C	3.650981	0.505564	5.009854
C	-6.166441	1.634486	-1.482257
C	-1.710505	-0.72371	3.403984
C	-1.629254	-1.463584	-4.67793
C	-0.669439	-4.85855	1.640355
H	-3.767614	2.255538	-2.769539
H	-3.925889	3.336523	-1.354244
H	-2.686752	2.053349	-1.357767
H	-6.247907	1.575034	-2.580212
H	-6.882996	0.92437	-1.038309
H	-6.460947	2.651958	-1.176011
H	-4.472315	0.3099	-1.404853
H	-5.372255	3.322395	0.69386
H	-5.124089	3.378175	3.172303
H	-4.185377	1.420107	4.377401
H	-1.221212	-1.605491	3.850269
H	-1.280402	-0.540517	2.409582
H	-1.490878	0.151626	4.03711
H	-3.419387	-2.146925	5.128442
H	-3.567797	-0.400979	5.424122
H	-4.929298	-1.29201	4.688325
H	-3.407001	-1.85661	2.720212
H	-5.391036	-2.181443	0.674023
H	-3.824017	-3.989476	-0.765539
H	0.783405	-2.773349	2.78375
H	1.78929	-3.495933	1.509046
H	1.120365	-1.859631	1.280281

H	-0.769019	-4.805454	2.737722
H	-1.605736	-5.265293	1.223644
H	0.147568	-5.55997	1.401958
H	-1.201411	-2.797493	1.335724
H	1.623174	-4.564486	-0.439835
H	1.797991	-4.719768	-2.918694
H	0.039562	-3.708885	-4.36322
H	-2.883327	-1.76521	-2.959085
H	-2.436345	-0.976812	-5.250094
H	-1.002802	-0.687078	-4.212008
H	-1.00714	-2.031224	-5.389476
H	-3.903302	-3.028694	-4.86705
H	-2.515857	-4.156815	-4.857998
H	-3.61607	-4.088758	-3.454462
H	1.134125	1.219517	4.071149
H	1.195905	0.338856	2.510348
H	1.269726	-0.561459	4.044521
H	3.261263	1.396397	5.528349
H	3.30832	-0.379279	5.57112
H	4.752287	0.531823	5.045291
H	3.385208	1.454291	3.103533
H	3.994598	-2.029562	4.324685
H	4.842136	-3.864906	2.882924
H	5.025215	-3.549171	0.426973
H	5.815478	-0.324739	-2.47126
H	5.804571	0.447209	-0.860185
H	6.630639	-1.12293	-1.093977
H	4.297458	-2.315343	-2.95024
H	5.221703	-3.217265	-1.724705
H	3.43474	-3.126055	-1.614542
H	3.602593	-0.634463	-1.354416
H	5.334534	1.945549	1.283445

H	3.903913	4.034954	0.114252
H	-1.116194	2.490267	3.015835
H	-1.966744	3.493027	1.823377
H	-1.491829	1.818058	1.406635
H	0.634049	4.297621	3.295407
H	1.656052	4.791664	1.91136
H	-0.04678	5.325725	1.999463
H	0.909099	2.42167	1.673084
H	3.953213	3.775882	-4.675131
H	2.209346	3.853556	-5.008995
H	2.96413	5.08264	-3.956037
H	3.590043	1.355527	-3.981853
H	2.574906	0.965606	-2.560465
H	1.803166	1.445577	-4.08764
H	3.599319	3.220289	-2.33968
H	-1.742387	4.359774	-0.141905
H	-1.629164	4.897658	-2.564794
H	0.413036	4.374194	-3.874437

Table S12. Cartesian geometry of $[(\text{GeNIPr})_2]^{2+}$ at B97-D/6-31G* level in Angstrom [\AA].

C	2.681733	-2.497593	-1.795727
C	2.406325	-2.921414	-0.473917
C	3.320327	-2.791824	0.600071
C	4.552307	-2.17456	0.313366
C	4.8504	-1.718418	-0.978494
C	3.931203	-1.88653	-2.021685
N	1.083267	-3.415234	-0.187383
C	0.003224	-2.590846	0.000062
N	-1.074848	-3.417751	0.187838
C	-0.665458	-4.75022	0.120763
C	0.677045	-4.748659	-0.119828
N	0.001582	-1.248412	-0.000131

Ge	-1.537598	-0.001911	-0.000213
N	-0.001559	1.248428	-0.000132
Ge	1.537619	0.00193	-0.000261
C	-2.3991	-2.926938	0.473987
C	-3.313115	-2.799627	-0.60027
C	-4.546502	-2.18496	-0.31402
C	-4.845899	-1.729113	0.977646
C	-3.926607	-1.894965	2.021112
C	-2.67577	-2.503426	1.79563
C	-2.957521	-3.257093	-2.015096
C	-2.293749	-2.099963	-2.800655
C	-1.696226	-2.698184	2.949482
C	-1.340723	-1.354112	3.621227
C	2.9661	-3.249916	2.015024
C	2.299216	-2.09441	2.800321
C	1.702339	-2.694678	-2.949294
C	2.28174	-3.688644	-3.984742
C	-0.003244	2.590861	0.000221
N	-1.083319	3.415219	-0.187184
C	-0.677163	4.748655	-0.119467
C	0.665332	4.750248	0.121172
N	1.074783	3.417791	0.188111
C	-2.406331	2.921343	-0.473828
C	-3.320397	2.791648	0.600096
C	-4.552313	2.174316	0.313281
C	-4.850276	1.718167	-0.978611
C	-3.931015	1.886367	-2.021727
C	-2.681617	2.497551	-1.79567
C	-2.966272	3.249676	2.015096
C	-4.180412	3.798469	2.795878
C	-1.70218	2.694794	-2.949179
C	-1.343534	1.351706	-3.621221

C	2.399048	2.926991	0.474202
C	2.675708	2.503324	1.79579
C	3.926568	1.894887	2.021224
C	4.845886	1.729206	0.977754
C	4.546492	2.185208	-0.313861
C	3.313083	2.799849	-0.600057
C	1.696137	2.69791	2.949648
C	1.340688	1.353752	3.621249
C	2.957525	3.257536	-2.014815
C	4.170041	3.810303	-2.795316
C	2.273635	3.692818	3.98525
C	2.293942	2.100479	-2.800639
C	-2.2816	3.688842	-3.984536
C	-2.299261	2.094194	2.800331
C	-4.170003	-3.809586	-2.795836
C	-2.273773	-3.693167	3.98498
C	4.180147	-3.79896	2.795778
C	1.343801	-1.351495	-3.621206
H	-2.044128	2.422149	3.820613
H	-2.985642	1.236222	2.87473
H	-1.370374	1.756333	2.312923
H	-3.835836	4.238121	3.743761
H	-4.710109	4.574396	2.222947
H	-4.896974	2.999244	3.043251
H	-2.229612	4.064387	1.937939
H	-5.288484	2.058149	1.107952
H	-5.813493	1.244782	-1.175975
H	-4.185703	1.559095	-3.030599
H	-0.599319	1.513379	-4.41588
H	-0.918876	0.642607	-2.893101
H	-2.230873	0.884192	-4.074911
H	-1.554003	3.853116	-4.794486

H	-3.207547	3.292955	-4.42993
H	-2.512623	4.659031	-3.518539
H	-0.771043	3.129017	-2.555985
H	-1.386785	5.556132	-0.254009
H	1.372953	5.559411	0.25613
H	2.037958	2.428194	-3.820784
H	2.982797	1.244518	-2.875384
H	1.365991	1.759724	-2.313493
H	3.8242	4.249216	-3.743082
H	4.697309	4.58765	-2.222073
H	4.889052	3.013343	-3.042874
H	2.218447	4.070016	-1.937268
H	5.282663	2.070972	-1.108814
H	5.810226	1.257903	1.174609
H	4.182293	1.56778	3.029887
H	0.763962	3.130249	2.556852
H	0.596136	1.513365	4.416007
H	0.917688	0.643846	2.892945
H	2.229183	0.888233	4.074713
H	1.545901	3.855185	4.795464
H	3.200571	3.298795	4.430239
H	2.502397	4.663694	3.51957
H	0.59964	-1.513035	-4.415942
H	0.919103	-0.642456	-2.893043
H	2.231201	-0.883962	-4.074757
H	1.554147	-3.852835	-4.794711
H	3.2077	-3.292747	-4.430097
H	2.512732	-4.658877	-3.518821
H	0.771166	-3.128896	-2.556177
H	4.185992	-1.559252	-3.030529
H	5.813666	-1.245099	-1.175782
H	5.288423	-2.058463	1.108096

H	3.835485	-4.238683	3.743599
H	4.709759	-4.574888	2.22277
H	4.896815	-2.999869	3.043275
H	2.043974	-2.422412	3.82056
H	2.985698	-1.236531	2.874831
H	1.370396	-1.756425	2.312867
H	2.229329	-4.064517	1.937783
H	1.386641	-5.556152	-0.254404
H	-1.373118	-5.559364	0.255629
H	-2.03773	-2.427512	-3.820845
H	-2.982519	-1.243924	-2.875293
H	-1.365783	-1.759391	-2.313398
H	-3.824079	-4.248463	-3.743586
H	-4.697486	-4.586908	-2.222758
H	-4.888849	-3.012494	-3.043449
H	-2.218539	-4.069673	-1.937629
H	-1.546035	-3.855674	4.795162
H	-3.20067	-3.299127	4.430035
H	-2.502613	-4.663977	3.519199
H	-0.596186	-1.513848	4.415975
H	-0.917685	-0.644149	2.893001
H	-2.229197	-0.888595	4.074737
H	-0.764063	-3.130516	2.55665
H	-5.282652	-2.070589	-1.108971
H	-5.810223	-1.257796	1.174549
H	-4.182346	-1.567962	3.029804

Table S13. Cartesian geometry of $3[\text{BF}_4]$ at B97-D/6-31G* level in Angstrom [\AA].

C	-1.861673	3.914811	-1.547627
C	-0.523309	3.452478	-1.548416
C	0.106842	2.8811	-2.684255
C	-0.659794	2.812339	-3.861134

C	-1.977735	3.289519	-3.902903
C	-2.57072	3.835431	-2.760702
N	0.215794	3.522752	-0.312539
C	0.478001	2.441637	0.496922
N	1.189078	2.942043	1.570944
C	1.334787	4.324021	1.435222
C	0.734112	4.682807	0.267164
N	0.086523	1.194478	0.305453
Ge	0.863191	-0.436133	0.950959
N	-0.858829	-1.136808	0.355305
Ge	-1.703763	0.558648	-0.527166
F	-2.634463	1.110853	0.955061
C	1.651905	2.132849	2.669266
C	3.032748	1.825909	2.739001
C	3.444744	0.969593	3.776956
C	2.519893	0.440094	4.68556
C	1.161883	0.771235	4.593582
C	0.692192	1.631626	3.583756
C	4.009078	2.342489	1.682154
C	5.477611	2.386094	2.150071
C	-0.775715	2.045121	3.513394
C	-1.743698	0.985016	4.072395
C	1.537264	2.334389	-2.626215
C	2.586798	3.464065	-2.48418
C	-2.537205	4.481448	-0.297331
C	-2.559286	6.028295	-0.349582
C	-1.214673	-2.400723	0.193465
N	-2.462031	-2.864649	-0.174183
C	-2.436326	-4.258242	-0.287485
C	-1.181306	-4.672114	0.036495
N	-0.435189	-3.535483	0.351616
C	-3.569886	-2.032624	-0.566308

C	-4.392748	-1.474992	0.442147
C	-5.478205	-0.690524	0.016919
C	-5.727948	-0.480775	-1.346771
C	-4.880291	-1.026498	-2.316994
C	-3.76455	-1.799204	-1.947402
C	-4.081925	-1.708418	1.921566
C	-4.709426	-0.652552	2.852029
C	-2.801068	-2.334649	-3.004964
C	-2.41781	-1.255382	-4.043286
C	0.997262	-3.456119	0.483879
C	1.569555	-3.573266	1.772751
C	2.9389	-3.272623	1.888254
C	3.682317	-2.859169	0.77186
C	3.097083	-2.794199	-0.499397
C	1.736586	-3.119678	-0.675245
C	0.713856	-3.971336	2.977269
C	1.51261	-4.733681	4.054983
C	1.115977	-3.097831	-2.069939
C	0.92747	-1.649637	-2.577526
C	-4.518341	-3.126736	2.363423
C	0.01799	-2.741296	3.608806
C	1.963933	-3.92925	-3.061955
C	-3.391016	-3.581514	-3.704549
C	3.890859	1.488066	0.39871
C	1.91281	1.445562	-3.828475
C	-3.970637	3.938615	-0.0995
C	-0.961045	3.403368	4.233333
H	4.565025	1.853473	-0.386153
H	4.161051	0.440895	0.597369
H	2.869356	1.507502	-0.004474
H	6.083996	2.892689	1.384456
H	5.589642	2.924123	3.105736

H	5.887221	1.370269	2.267963
H	-2.011111	3.730308	4.156089
H	-0.699527	3.315219	5.301002
H	-0.321049	4.180223	3.784136
H	-2.774527	1.292244	3.851362
H	-1.57349	0.009387	3.593653
H	-1.645944	0.870401	5.165206
H	-3.036691	6.432756	0.558059
H	-1.544866	6.449841	-0.426097
H	-3.135045	6.370591	-1.225269
H	-4.359017	4.292044	0.869421
H	-4.649794	4.30841	-0.884751
H	-3.980287	2.840635	-0.098683
H	3.587751	3.011744	-2.417469
H	2.559295	4.120798	-3.369563
H	2.421292	4.080085	-1.588362
H	2.867136	0.939385	-3.627225
H	1.151149	0.673525	-4.011228
H	2.024401	2.049752	-4.74509
H	-1.638734	-1.652874	-4.712153
H	-3.282682	-0.971181	-4.664191
H	-2.030796	-0.351863	-3.54878
H	-2.68025	-3.967786	-4.453187
H	-3.603131	-4.383854	-2.980085
H	-4.332036	-3.325899	-4.218681
H	-4.262411	-3.283651	3.424446
H	-5.609574	-3.240222	2.252244
H	-4.025054	-3.911932	1.772042
H	-4.323208	-0.792968	3.873334
H	-4.454377	0.36075	2.51427
H	-5.806701	-0.757474	2.891755
H	-0.58606	-3.050409	4.478765

H	0.767753	-2.008084	3.945999
H	-0.649505	-2.242256	2.891062
H	0.824551	-5.115678	4.825716
H	2.065008	-5.582705	3.622566
H	2.237411	-4.070269	4.554247
H	1.432555	-3.991709	-4.026167
H	2.937309	-3.454441	-3.241703
H	2.122347	-4.951514	-2.681035
H	0.631474	-1.660779	-3.63869
H	0.128927	-1.144721	-2.012874
H	1.850763	-1.066222	-2.474757
H	1.598265	1.700414	-1.728854
H	-0.22027	2.372738	-4.755253
H	-2.54667	3.225506	-4.833071
H	-3.602332	4.187125	-2.798747
H	-1.95328	4.176826	0.583959
H	3.716715	3.373358	1.424632
H	4.497791	0.705585	3.867087
H	2.860622	-0.233855	5.474772
H	0.456198	0.356803	5.313001
H	-1.057766	2.182922	2.463485
H	-1.871824	-2.64305	-2.503744
H	-5.065562	-0.829836	-3.373483
H	-6.579213	0.131503	-1.652075
H	-6.126651	-0.224866	0.75779
H	-2.989831	-1.630056	2.036878
H	0.119117	-3.566843	-2.021428
H	-0.080859	-4.644898	2.616373
H	3.42506	-3.347064	2.86179
H	4.737613	-2.601068	0.87604
H	3.702451	-2.500466	-1.355829
H	-0.733726	-5.657616	0.075664

H	-3.324717	-4.803916	-0.57828
H	0.641756	5.63967	-0.229098
H	1.869452	4.902964	2.17764
B	5.2021	-0.938258	-2.972739
F	5.744872	-2.075261	-2.294843
F	6.065698	-0.485042	-3.979786
F	3.934431	-1.317747	-3.540002
F	4.965699	0.097678	-2.012926

Table S14. Cartesian geometry of $\text{BF}_3 \cdot \text{OEt}_2$ at B97-D/6-31G* level in Angstrom [Å].

B	0.399345	-1.122127	0.053989
F	1.584127	-1.283568	-0.605861
F	0.49538	-0.93452	1.413003
F	-0.618178	-1.948028	-0.350254
O	-0.141964	0.483264	-0.52913
C	-1.585389	0.626603	-0.774924
H	-1.707376	1.580774	-1.311302
H	-1.829971	-0.201	-1.448318
C	-2.417567	0.575782	0.504671
H	-3.48489	0.637091	0.237482
H	-2.24018	-0.368026	1.037853
H	-2.18341	1.417256	1.174002
C	0.438499	1.644009	0.166553
C	1.951917	1.657757	-0.003591
H	-0.019503	2.532391	-0.295652
H	0.148197	1.591242	1.225163
H	2.337884	2.589379	0.441218
H	2.418737	0.804326	0.503297
H	2.22278	1.631227	-1.068893

Table S15. Cartesian geometry of OEt₂ at B97-D/6-31G* level in Angstrom [Å].

C	2.083687	0.613203	-0.166957
C	1.254149	-0.628256	0.202654
O	-0.076429	-0.60209	-0.315432
C	-0.928195	0.315152	0.370235
C	-2.348089	0.132386	-0.164776
H	1.229599	-0.753314	1.306055
H	1.715999	-1.529796	-0.230387
H	3.121936	0.492384	0.184074
H	2.093463	0.749924	-1.259672
H	1.67328	1.524817	0.295112
H	-0.894223	0.117217	1.463222
H	-0.592953	1.360201	0.215426
H	-3.037613	0.826147	0.342625
H	-2.376788	0.333922	-1.246791
H	-2.690579	-0.899696	0.006855

4.) Supplementary References

- [S1] T. Ochiai, D. Franz, X.-N. Wu, S. Inoue, *Dalton Trans.* **2015**, *44*, 10952.
- [S2] G. M. Sheldrick, *SHELX-97 Program for Crystal Structure Determination*, Universität Göttingen (Germany) **1997**.
- [S3] (a) C. Lee, W. Yang, R. G. Parr, *Phys. Rev. B* **1988**, *37*, 785. (b) A. D. Becke, *J. Chem. Phys.* **1993**, *98*, 5648.
- [S4] (a) G. A. Petersson, M. A. Al-Laham, *J. Chem. Phys.* **1991**, *94*, 6081. (b) J.-P. Blaudeau, M. P. McGrath, L. A. Curtiss, L. Radom, *J. Chem. Phys.* **1997**, *107*, 5016.
- [S5] (a) A. D. Becke, *J. Chem. Phys.* **1997**, *107*, 8554. (b) S. Grimme, *J. Comput. Chem.* **2006**, *27*, 1787.
- [S6] Gaussian 09, Revision B.01, M. J. Frisch, G. W. Trucks, H. B. Schlegel, G. E. Scuseria, M. A. Robb, J. R. Cheeseman, G. Scalmani, V. Barone, B. Mennucci, G. A. Petersson, H. Nakatsuji, M. Caricato, X. Li, H. P. Hratchian, A. F. Izmaylov, J. Bloino, G. Zheng, J. L. Sonnenberg, M. Hada, M. Ehara, K. Toyota, R. Fukuda, J. Hasegawa, M. Ishida, T. Nakajima, Y. Honda, O. Kitao, H. Nakai, T. Vreven, J. A. Montgomery, Jr. J. E. Peralta, F. Ogliaro, M. Bearpark, J. J. Heyd, E. Brothers, K. N. Kudin, V. N. Staroverov, R. Kobayashi, J. Normand, K. Raghavachari, A. Rendell, J. C. Burant, S. S. Iyengar, J. Tomasi, M. Cossi, N. Rega, N. J. Millam, M. Klene, J. E. Knox, J. B. Cross, V. Bakken, C. Adamo, J. Jaramillo, R. Gomperts, R. E. Stratmann, O. Yazyev, A. J. Austin, R. Cammi, C. Pomelli, J. W. Ochterski, R. L. Martin, K. Morokuma, V. G. Zakrzewski, G. A. Voth, P. Salvador, J. J. Dannenberg, S. Dapprich, A. D. Daniels, Ö. Farkas, J. B. Foresman, J. V. Ortiz, J. Cioslowski, D. J. Fox, Gaussian, Inc., Wallingford CT, **2009**.